# Discovery of a Potent and Selective Prostaglandin D 2 Receptor Antagonist, [(3 R )-4-(4-Chloro-benzyl)-7-fluoro-5-(methylsulfonyl)-1,2,3,4-tetrahydrocyclopenta[ b ]indol-3-yl]-ace...

**ARTICLE** *in* JOURNAL OF MEDICINAL CHEMISTRY · MARCH 2007

Impact Factor: 5.45 · DOI: 10.1021/jm0603668 · Source: PubMed

# Discovery of a Potent and Selective Prostaglandin $D_2$ Receptor Antagonist, [(3*R*)-4-(4-Chlorobenzyl)-7-fluoro-5-(methylsulfonyl)-1,2,3,4-tetrahydrocyclopenta[*b*]indol-3-yl]-acetic Acid (MK-0524)†

Claudio F. Sturino,*,‡ Gary O'Neill,*,§ Nicolas Lachance,‡ Michael Boyd,‡ Carl Berthelette,‡ Marc Labelle,‡ Lianhai Li,‡ Bruno Roy,‡ John Scheigetz,‡ Nancy Tsou,⊥ Yves Aubin,‡ Kevin P. Bateman,‡ Nathalie Chauret,‡ Stephen H. Day,‡ Jean-François Lévesque,‡ Carmai Seto,‡ Jose H. Silva,‡ Laird A. Trimble,‡ Marie-Claude Carriere,§ Danielle Denis,§ Gillian Greig,§ Stacia Kargman,§ Sonia Lamontagne,§ Marie-Claude Mathieu,§ Nicole Sawyer,§ Deborah Slipetz,§ William M. Abraham,|| Tom Jones,▽ Malia McAuliffe,▽ Hana Piechuta,▽ Deborah A. Nicoll-Griffith,‡ Zhaoyin Wang,‡ Robert Zamboni,‡ Robert N. Young,‡ and Kathleen M. Metters§

*Department of Medicinal Chemistry, Merck Frosst Canada & Co., 16711 Trans Canada Highway, Kirkland, Quebec H9H 3L1, Canada, Department of Biochemistry, Merck Frosst Canada & Co., 16711 Trans Canada Highway, Kirkland, Quebec H9H 3L1, Canada, Department of Medicinal Chemistry, Merck Research Laboratories, PO Box 2000, Rahway, New Jersey 07065, Miller School of Medicine, University of Miami at Mount Sinai Medical Center, 430 Alton Road, Miami Beach, Florida 33140, and Department of Pharmacology, Merck Frosst Canada & Co., 16711 Trans Canada Highway, Kirkland, Quebec H9H 3L1, Canada*

*Received March 29, 2006*

The discovery of the potent and selective prostaglandin $D_2$ ($PGD_2$) receptor (DP) antagonist [(3*R*)-4-(4-chlorobenzyl)-7-fluoro-5-(methylsulfonyl)-1,2,3,4-tetrahydrocyclopenta[*b*]indol-3-yl]-acetic acid **(13)** is presented. Initial lead antagonists **6** and **7** were found to be potent and selective DP antagonists (DP $K_i$ = 2.0 nM for each); however, they both suffered from poor pharmacokinetic profiles, short half-lives and high clearance rates in rats. Rat bile duct cannulation studies revealed that high concentrations of parent drug were present in the biliary fluid ($C_{max}$ = 1100 $\mu$M for **6** and 3900 $\mu$M for **7**). This pharmacokinetic liability was circumvented by replacing the 7-methylsulfone substituent present in **6** and **7** with a fluorine atom resulting in antagonists with diminished propensity for biliary excretion and with superior pharmacokinetic profiles. Further optimization led to the discovery of the potent and selective DP antagonist **13**.

## Introduction

Seasonal allergic rhinitis is an upper-airway disorder that typically results in nasal congestion, itching, and rhinorrhea. Histamine, cysteinyl leukotrienes (CysLTs), thromboxane $A_2$ ($TxA_2$), and prostaglandin $D_2$ ($PGD_2$) are considered key mediators in allergic rhinitis, as well as in other allergic conditions such as allergic asthma, atopic dermatitis, and allergic conjunctivitis.[1] Release of the above mediators in response to IgE-dependent stimuli results in an increase in mucus production and intranasal pressure. Leukotriene $D_4$ receptor antagonists and antihistamines have shown efficacy in a guinea pig model of allergic rhinitis and conjunctivitis.[2] While antihistamines are able to control the symptoms of the early allergic response, namely, sneezing, itching, and rhinorrhea, they are less effective at treating symptoms of the late allergic reaction such as nasal congestion. Even though a number of treatment options are available today to treat allergic rhinitis, there still remains a medical need for an orally dosed nasal decongestant with a better side-effect profile than what is currently available.

In response to IgE-dependent stimuli, $PGD_2$ is the major cyclooxygenase-derived metabolite obtained from the degranulation of mast cells.[3] $PGD_2$ is thought to mediate the nasal congestion associated with allergic rhinitis by causing vasodilation in the nasal mucosa.[4] It has been reported that nasal challenge with $PGD_2$ in humans results in a dose-dependent increase in nasal congestion. This $PGD_2$-induced nasal congestion was produced with approximately 10-fold greater potency than histamine and with 100-fold greater potency than bradykinin.[5] In addition to the above finding, it has also been reported that elevated levels of $PGD_2$ were measured in the nasal washings of allergic patients that underwent a nasal antigen challenge.[6] Also, DP[a] knockout mice have been shown to exhibit a reduced allergic response with no obvious abnormalities.[7] $PGD_2$ and its receptor (DP receptor) have been implicated in a number of physiological processes such as regulation of body temperature, sleep, and pain.[8] The implication that $PGD_2$ is involved in allergic diseases has prompted us to identify a suitable clinical $PGD_2$ receptor antagonist to treat the inflammatory effects exerted through the actions of $PGD_2$.[9]

We have recently reported on an indole series of DP receptor antagonists.[10a] In particular, indoles **6** and **7** were noted to be potent and selective DP antagonists. Unfortunately, these antagonists displayed poor pharmacokinetic profiles that excluded them from being potential clinical candidates. In this paper, we wish to highlight some of the medicinal chemistry issues, principally related to pharmacokinetics and metabolism, that were addressed during the optimization of an indole series of DP antagonists leading eventually to the identification of the potent and selective $PGD_2$ receptor antagonist **13**.[10b]

To date, there has been no reported clinical experience with the use of DP antagonists in the treatment of airway diseases.

† The x-ray crystallographic data for compound **14** has been deposited with the Cambridge Crystallographic Data Centre (CCDC601363).

* Corresponding authors. C.F.S.: tel (514) 428-2630, fax (514) 428-4900, e-mail claudio_sturino@merck.com. G.O.: tel (514) 428-7920, fax (514) 428-4900, e-mail gary_oneill1@merck.com.

‡ Department of Medicinal Chemistry, Merck Frosst Canada & Co.

§ Department of Biochemistry, Merck Frosst Canada & Co.

⊥ Department of Medicinal Chemistry, Merck Research Laboratories.

|| University of Miami at Mount Sinai Medical Center.

▽ Department of Pharmacology, Merck Frosst Canada & Co.

[a] Abbreviations: DP, $PGD_2$ receptor; TP, $TxA_2$ receptor; $EP_{1-4}$, $PGE_2$ receptor subtypes 1, 2, 3, and 4; FP, $PGF_{2\alpha}$ receptor; IP, $PGI_2$ receptor.

10.1021/jm0603668 CCC: $37.00 
Published on Web 01/20/2007

**Scheme 1.** Synthesis of 7-Methylsulphone Indole Series of DP Receptor Antagonists[a]

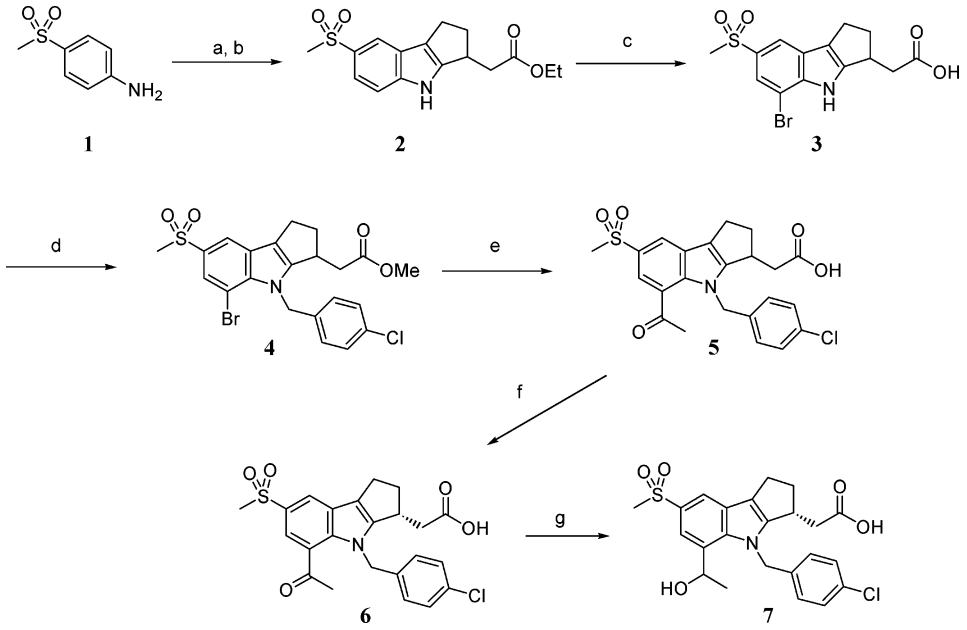


[a] (a) $I_2$, $Ag_2SO_4$, EtOH; (b) (i) $(EtO)_4Si$, PPTS, ethyl 2-(2-oxocyclopentyl)acetate, 130−140 °C, 6 h; (ii) $^iPr_2NEt$, $Pd(OAc)_2$, DMF, 120 °C, 2 h; (c) (i) 2 N NaOH, MeOH, THF, 60 °C; (ii) PyrHBr·$Br_2$, pyr, −25 °C to rt; (iii) Zn, AcOH, 10 °C; (d) (i) $CH_2N_2$, $Et_2O$, THF; (ii) NaH, 4-chlorobenzyl bromide, DMF; (e) (i) 1-ethoxyvinyltributyltin, $Pd_2(dba)_3$, $Ph_3As$, DMF, 80 °C; (ii) 2 N HCl; (iii) 2 N NaOH, THF, MeOH; (f) chiral HPLC separation of enatiomers; (g) (i) $NaBH_4$, MeOH; (ii) chiral HPLC separation.

Recently, the use of the $PGD_2$ receptor antagonist **13** for the suppression of nicotinic acid-induced vasodilation in humans has been reported.[11]

## Chemistry

The synthetic routes developed for the synthesis of the DP receptor antagonists are outlined in Schemes 1 and 2. Iodination of 4-methylsulfonylphenylamine (**1**) with iodine and silver sulfate in ethanol[12] cleanly afforded the 2-iodo adduct in 80% yield. This aniline was then condensed with 2-(2-oxocyclopentyl)acetate in the presence of tetraethoxysilane as a dehydrating reagent and with catalytic quantities of pyridinium *p*-toluenesulfonate (PPTS). The resulting imine was then treated with $Pd(OAc)_2$ and Hunig's base in DMF to afford the corresponding indole in 39% overall yield.[13] Introduction of the 7-bromo substituent was accomplished by first hydrolyzing the ester to the acid followed by reaction with pyridinium perbromide in pyridine[14] (see Figure 1 for numbering of the 1,2,3,4-tetrahydrocyclopenta[*b*]indole ring system). This reaction is believed to result in the introduction of three bromine atoms to the indole ring system, namely, at the 3a, 5, and 8b positions. Zinc treatment of this intermediate serves to eliminate the bromides at the 3a and 8b positions and delivers the monobromo adduct **3** in 81% overall yield. It is worth noting that attempts at brominating ester **2** under similar reaction conditions proved unsuccessful. Acid **3** was subsequently esterified with diazomethane and then treated with NaH in DMF followed by 4-chlorobenzyl bromide to cleanly generate the benzyl derivative in 89% yield. The 5-bromo substituent in turn was converted into a methyl ketone by first performing a Stille cross coupling reaction with 1-ethoxyvinyltributyltin employing $Pd_2(dba)_3/Ph_3As$ (dba = dibenzylideneacetone) as the catalyst system.[15] The resulting vinyl ether was hydrolyzed to the corresponding ketone **5**. This acid was resolved into its individual enantiomers by HPLC separation on chiral support to deliver enantiomer **6**. Standard reduction of **6** employing $NaBH_4$ in MeOH, followed by HPLC separation on chiral support of the two diasastereomeric alcohols delivered **7** as a single diastereomer.

The synthesis of **13** is outlined in Scheme 2 and incorporates similar transformations as described above. 4-Fluorophenylamine (**8**) was iodinated,[16] and following palladium mediated indole synthesis, the adduct **9** was obtained in moderate yield. For large scale preparation of **9**, it was more convenient to make use of the commercially available 2-bromo-4-fluoroaniline as starting material as outlined in Scheme 2. Bromination of **9**, followed by benzylation, proceeded to deliver acid **10**. The resolution of this material was accomplished by recrystallization of its (*S*)-(−)-1-(napthyl)ethylamine salt. This procedure conveniently provided the resolved acid **11** after acid workup. Bromide **11** was then transformed into the corresponding methylketone **12** as described. For the introduction of the methylsulfone, as required in **13**, acid **11** was first esterified with diazomethane and then treated with methanesulfinic acid sodium salt and CuI in *N*-methylpyrrolidone (NMP) at 150 °C for 3 h.[17] These conditions were found to cleanly convert the aryl bromide into a methylsulfone in high yields. Standard hydrolysis thus delivered the DP antagonist **13**. It is worth noting that this sulfonylation reaction tolerates an acid functional group because treatment of the free acid **11** under identical conditions delivered **13** with comparable yields. The absolute stereochemistry of the acetic acid side chain present in **11**, **12**, and **13** was established to be (*R*) from a single-crystal X-ray analysis of the acid intermediate **14**.[18]

## Results and Discussion

We have recently disclosed the *in vitro* prostanoid receptor binding profiles of antagonists **6** and **7**. Both of these compounds are potent DP antagonists with $K_i$ values of 2.6 ± 0.7 and 1.8 ± 0.7 nM for **6** and **7**, respectively (Table 1).[19] The stereochemistry of the acetic acid side chain (stereochemistry (*R*)) is critical for activity because the corresponding (*S*) stereoisomers are generally greater than 100-fold less active on the DP receptor. The stereochemistry at the alcohol center of **7** is also important for DP activity because the corresponding diastereomeric alcohol was found to be less potent ($K_i$ = 8.9 ± 1.8 nM, $n$ = 4). Antagonists **6** and **7** are also selective for the remaining

**Scheme 2.** Synthesis of 7-Fluoro Indole Series of DP Receptor Antagonists[a]

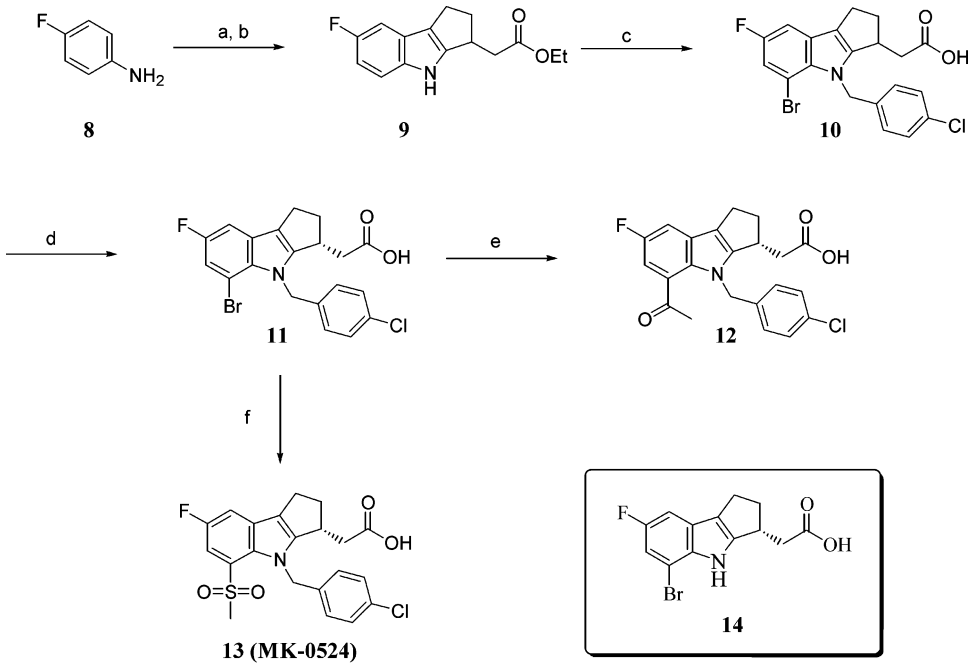


[a] (a) $I_2$, $NaHCO_3$, $H_2O$, toluene; (b) (i) $(EtO)_4Si$, PPTS, ethyl 2-(2-oxocyclopentyl)acetate; (ii) $^iPr_2NEt$, $Pd(OAc)_2$, DMF; (c) (i) 2 N NaOH, MeOH, THF; (ii) PyrHBr·$Br_2$, pyr, −25 °C to rt; (iii) Zn, AcOH, 10 °C; (iv) HCl, MeOH; (v) NaH, 4-chlorobenzyl bromide, DMF; (vi) 2 N NaOH, THF, MeOH; (d) (i) (*S*)-(−)-1-(napthyl)ethylamine, MeOH; (ii) recrystallize, EtOH; (iii) 1 N HCl; (e) (i) $CH_2N_2$, $Et_2O$, THF; (ii) 1-ethoxyvinyltributyltin, $Pd_2(dba)_3$, $Ph_3As$, DMF, 90 °C; (iii) 1 N HCl; (iv) 1 N NaOH, THF, MeOH; (f) (i) $CH_2N_2$, $Et_2O$, THF; (ii) $MeSO_2Na$, CuI, NMP, 150 °C, 3 h; (iii) 2 N NaOH, THF, MeOH; (g) (i) ethyl 2-(2-oxocyclopentyl)acetate, toluene, *p*-TsOH·$H_2O$, reflux; (ii) $Pd(OAc)_2$, KOAC, $^nBu_4NCl$, DMF, 80 °C.

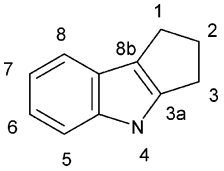


16

**Figure 1.** 1,2,3,4-Tetrahydrocyclopenta[*b*]indole numbering system.

prostanoid receptors (TP, $EP_{1-4}$, FP, and IP, see Table 1)[20] with alcohol **7** exhibiting higher selectivity versus the TP receptor than ketone **6**. In addition, these compounds are potent antagonists in DP functional assays where they inhibit the production of $PGD_2$-induced cyclic adenosine monophosphate (cAMP) in washed platelets (WP) ($IC_{50}$ of 2 nM for both **6** and **7**) and in platelet-rich plasma (PRP) ($IC_{50}$ values of 7.9 ± 2.8 and 8.5 ± 4.3 nM for **6** and **7**, respectively). The high degree of selectivity was maintained versus TP in the functional assay as demonstrated from the TP PRP aggregation functional assay (Table 2, see Experimental Procedures for details of the functional assays), in agreement with the receptor binding profiles for these compounds.

Given the excellent *in vitro* profiles of **6** and **7**, the pharmacokinetic properties of these antagonists were evaluated in Sprague−Dawley rats, and the results are summarized in Table 3. Several points from Table 3 are worth discussing. While the bioavailability of **6** in rats is good, the bioavailability for antagonist **7** is not (8%). In addition, the maximum concentration ($C_{max}$) achieved with **6** is significantly higher than that with **7** (23 vs 0.29 $\mu$M at a dose of 10 mg/kg).[21] Even though the bioavailabilities of these antagonists in rats differ, they both exhibited short half-lives and high clearance rates (Table 3). Pharmacokinetic studies with **6** and **7** in other species (mouse, dog, cynomolgus monkey) also indicated that these antagonists displayed unsuitable pharmacokinetic profiles (short half-life, high clearance rates) that precluded them from being potential clinical candidates and underscored the need to identify other DP antagonists with improved pharmacokinetic profiles.

In an effort to investigate whether the rapid clearance of antagonists **6** or **7** was the result of drug metabolism, these compounds were incubated in a rat hepatocyte preparation and, after a 2 h period, the percent of parent drug remaining was determined for each compound.[22] Interestingly, as shown in Table 4, antagonists **6** and **7** were, in fact, not extensively metabolized with 93−100% of parent drug remaining at the end of the incubation period. The low metabolic turnover of these antagonists suggested to us that the rapid clearance in rats was likely not driven by Phase I or II metabolism. At this time, we elected to perform a rat bile duct cannulation study to determine what drug-derived compounds were being excreted into the biliary fluid in a hope that this would shed some light on the clearance pathways operative for **6** and **7**.[23] These experiments proved quite valuable. In these experiments, a cannula was inserted into the bile duct of anesthetized rats and,

**Table 1.** Prostanoid Receptor Binding Affinities, $K_i$ (nM)[a]

| compd | DP | TP | $EP_1$ | $EP_2$ | $EP_3$ | $EP_4$ | FP | IP |
|---|---|---|---|---|---|---|---|---|
| **6** | 2.6 ± 0.71 | 1200 ± 470 | >20000 | 230 ± 110 | >20000 | >20000 | >20000 | >20000 |
| **7** | 1.8 ± 0.70 | 7100 ± 820 | >20000 | 390 ± 33 | >20000 | >20000 | >20000 | >20000 |
| **11** | 1.5 ± 0.57 | 0.84 ± 0.19 | 4400 ± 1600 | 410 ± 320 | 470 ± 46 | 4400 ± 1500 | 14000 ± 3100 | 400 ± 100 |
| **12** | 1.1 ± 0.22 | 14 ± 2.7 | >9000 | 310 ± 82 | 1200 ± 260 | >20000 | >20000 | 14000 ± 2100 |
| **13** | 0.57 ± 0.17 | 2.95 ± 0.46 | 1160 ± 420 | 136 ± 8.0 | 892 ± 250 | >15200 | 9991 ± 5826 | 6628 ± 1343 |

[a] Values are means from at least three experiments.

**Table 2.** DP and TP Receptor Functional Activity in PRP and WP Assay[a]

| compd | DP WP $IC_{50}$, nM[b] | DP PRP $IC_{50}$, nM[c] | TP PRP $IC_{50}$, nM[d] |
|---|---|---|---|
| **6** | 2.0 ± 0.7 | 7.9 ± 2.8 | 8400 ± 4700 |
| **7** | 2.0 ± 1.4 | 8.6 ± 4.3 | 43000 ± 16000 |
| **11** | 0.26 ± 0.04 | 23 ± 9.5 | 80 ± 60 |
| **12** | 0.29 ± 0.05 | 15 ± 0.41 | 1400 ± 1000 |
| **13** | 0.09 ± 0.02 | 4.0 ± 0.9 | 770 ± 490 |

[a] Values are means from at least three experiments. $IC_{50}$ = concentration at which process is inhibited by 50%. [b] DP WP assay involved inhibition of the accumulation of cAMP in washed platelets challenged with $PGD_2$. [c] DP PRP assay involved inhibition of the accumulation of cAMP in platelet-rich plasma challenged with $PGD_2$. [d] TP PRP assay involved the inhibition of U44619-induced platelet aggregation in platelet-rich plasma.

**Table 3.** Rat Pharmacokinetic Parameters of DP Antagonists[a]

| compd | $F$ (%) | $C_{max}$, μM (10 mg/kg) | $C_{6h}$, μM (10 mg/kg) | $T_{1/2}$, h[e] | Clp (mL/min) | $V_{dss}$ |
|---|---|---|---|---|---|---|
| **6**[b] | 128 | 21 | 0.6 | 1.4 | 14 | 0.7 |
| **7**[b] | 8 | 0.29 | 0.03 | <1 | 50 | 0.8 |
| **11**[c] | 41 | 10 | 3.7 | 12 | 1.4 | 0.4 |
| **12**[d] | 52 | 21 | 7.5 | 4 | 1.9 | 0.5 |
| **13**[b] | 79 | 39 | 6.3 | 7 | 2.4 | 0.5 |

[a] The corresponding sodium salts were used for these pharmacokinetic studies. Half-lives are determined from the intravenous (iv) data. $F$ denotes bioavailability; $C_{max}$ denotes the maximum concentration reached; $C_{6h}$ denotes the concentration 6 h after dosing; $T_{1/2}$ is the half-life in plasma; Clp is plasma clearance; $V_{dss}$ is the volume of distribution. [b] Oral (po) dose 10 mg/kg, vehicle 0.5% methocel, dose volume 10 mL/kg, $n = 2$; iv dose 5 mg/kg, vehicle 5% dextrose, dose volume 1 mL/kg, $n = 2$. [c] po dose 5 mg/kg, vehicle 0.5% methocel, dose volume 10 mL/kg, $n = 2$; iv dose 5 mg/kg, vehicle 60% PEG 200, $n = 2$. [d] po dose 10 mg/kg, vehicle 60% PEG 200, dose volume 10 mL/kg, $n = 2$; iv dose 5 mg/kg, vehicle 60% PEG 200, dose volume 1 mL/kg, $n = 2$. [e] $T_{1/2}$ values were determined from the iv experiments.

**Table 4.** Metabolic Stability of DP Antagonists in Rat Hepatocyte Incubations[a]

| compd | percent parent remaining in rat hepatocytes (50 μM, 2 h incubation) |
|---|---|
| **6** | 93 |
| **7** | 100 |
| **11** | 42 |
| **12** | 35 |
| **13** | 32 |

[a] 0.5 mL of $2 \times 10^6$ cells/mL, 37 °C; 95/5 $O_2/CO_2$.

subsequently, antagonists **6** and **7** were administered intravenously. Bile fluid was collected in 30 min intervals and analyzed by HPLC-UV. As summarized in Table 5, these experiments revealed that the major drug-derived compound present in the bile fluid was, in fact, intact parent. We were particularly intrigued by the high levels of parent in the biliary fluid, 1100 μM for **6** and 3900 μM for antagonist **7**. These high drug levels confirmed that the major elimination pathway for antagonists **6** and **7** in rats was via biliary excretion. This mechanism is also consistent with the *in vitro* rat hepatocyte data (Table **4)** suggesting that the metabolism was not playing a significant role in the clearance of these DP antagonists. In addition, given

**Table 5.** Rat Biliary Concentrations of DP Antagonists[a]

| compd | $C_{max}$ of parent, μM | $t_{max}$ of parent, h |
|---|---|---|
| **6**[b] | 1100 | 0−0.5 |
| **7**[b] | 3900 | 0−0.5 |
| **11**[c] | 29 | 1−1.5 |
| **12**[c] | 81 | 2.5−3 |
| **13**[b] | 103 | 0.5−1 |

[a] The corresponding sodium salts were used for these pharmacokinetic studies. The compounds were administered iv at 5 mg/kg at a dose volume of 1 mL/kg; $n = 2$ for all studies except for **13** with $n = 5$. $C_{max}$ = maximum concentration; $t_{max}$ = time to reach maximum concentration. [b] iv, vehicle 5% dextrose. [c] iv, vehicle 60% PEG 200.

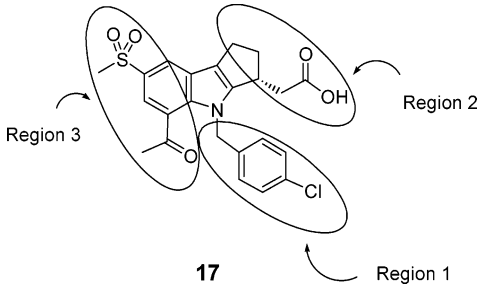


**Figure 2.** Medicinal chemistry strategy to elucidate biliary excretion SAR.

the high biliary levels of **6** and **7**, we speculate that this process is occurring via an active transport mechanism.[24]

To address the pharmacokinetic liability of the above DP antagonists, SAR studies were focused on identifying an analog of **6** or **7** that maintained the DP activity of these antagonists but with diminished propensity for biliary excretion. At the outset, this objective was derived from the hypothesis that reduced biliary excretion would result in improved pharmacokinetic (PK) profiles. Figure 2 highlights the medicinal chemistry strategy that was undertaken to identify compounds with diminished propensity for biliary excretion. We elected to divide the molecule into three distinct regions, as illustrated, modify in turn the different regions of the molecule, and evaluate any analog that displayed good DP potency for their rat PK profile. We initially examined the effects of replacing the 4-chlorobenzyl substituent of the molecule (region 1), and a number of replacements were examined including differentially substituted benzyl groups, alkyl substituents, benzothiazole, and quinoline. In general, these modifications led to compounds with either significantly diminished DP activity or comparable rat pharmacokinetic profiles to antagonist **6**. We next turned our attention to modifying region 2 of the molecule. Modifications at this region revealed that the carboxylic acid, the (*R*) stereochemistry, and the acetic acid are all required for DP activity. Concurrently, we also examined the benzenoid region of the molecule (region 3). A number of replacements were evaluated for the methylsulfone and ketone substituents, and of the various modifications examined, the most dramatic effect was seen when the methylsulfone group was replaced with a fluorine atom, leading to antagonists such as **11** and **12**.

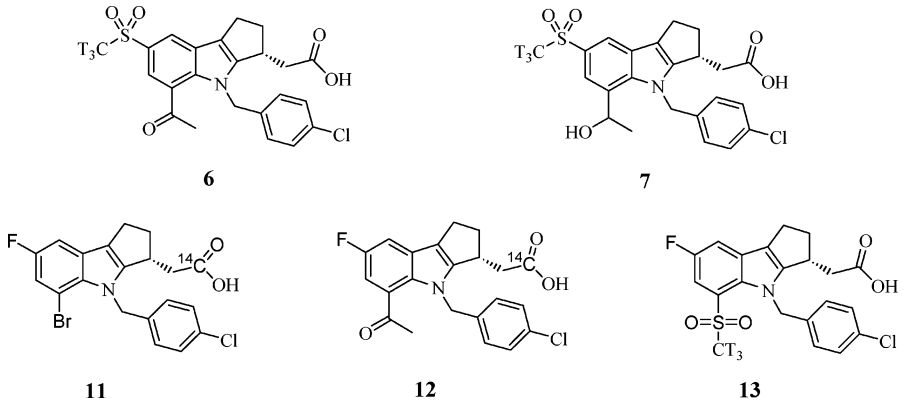

**Figure 3.** Radiolabeled DP antagonists.

Several properties of **11** and **12** are worth commenting. In terms of prostanoid receptor binding profiles, the fluoro analogs **11** and **12** remain potent DP antagonists although their selectivity versus the TP receptor is significantly diminished (see Table 1). This decrease in TP selectivity, as measured by the competition receptor binding assay, is evident when comparing the TP selectivity of the 7-fluoro indole **12** (selectivity = 13) versus the corresponding methylsulfone analog **6** (selectivity = 460, Table 1). As expected, this decreased TP selectivity in the binding assay translates to a decreased selectivity in the functional assay as well (Table 2). While the TP selectivity of the fluoro analogs is lower relative to the methylsulfone antagonists, the advantage of the 7-fluoro series becomes evident when one considers their pharmacokinetic properties. First, in terms of metabolic stability, as measured by the *in vitro* hepatocyte assay, the fluoro antagonists **11** and **12** are significantly *more* metabolized (42% and 35% parent remaining, respectively) than the methylsulfone analog **6** or **7** (93% and 100% parent remaining, respectively). However, the metabolically more labile fluorine analogs **11** and **12** displayed superior rat pharmacokinetic profiles as illustrated in Table 3. Antagonists **11** and **12** have good rat half-lives (12 and 4 h for **11** and **12**, respectively), decreased clearance rates, and similar volumes of distribution relative to the methylsulfone analogs. This improvement in pharmacokinetic profile results in higher plasma drug levels at 6 h as noted in Table 3. Rat bile duct cannulation studies with the fluoro antagonists **11** and **12** revealed that significantly lower levels of parent compound were present in the bile fluid (29 and 81 $\mu$M for **11** and **12**, respectively) than was observed with **6** or **7** (Table 5). In particular, the difference in the biliary excretion observed between antagonists **6** and **12** is quite notable. Replacing the methylsulfone substituent in **6** with a fluorine atom decreased the biliary $C_{max}$ from 1100 to 81 $\mu$M, a 13.6-fold decrease. It is also worth highlighting that the extent of metabolic turnover in the rat hepatocyte assay was not predictive of their *in vivo* pharmacokinetic profile due to the extensive biliary excretion of antagonist **6** and **7** versus the fluoro analogs **11** and **12**. At this point, antagonist **12** displayed an attractive *in vitro* and PK profile, and the focus of the medicinal chemistry effort was directed at trying to improve its activity in the functional assay ($IC_{50}$ in PRP assay of 15 nM).

Additional SAR studies, focusing primarily on the 5-position of the tetrahydrocyclopenta[*b*]indole, revealed that indeed it was possible to further improve the potency of the DP antagonists. A number of 5-position replacements were evaluated, including aryl, thiophene, heterocycles, and alkyl groups, and from these studies, the 5-methylsulfone **13** was identified. Antagonist **13** is a potent DP antagonist with a $K_i$ of 0.57 nM in the receptor binding assay. It is 5.2-fold selective versus the TP receptor in the binding assay, 239-fold selective versus $EP_2$ and >1500-fold selective against the remaining prostanoid receptors (Table 1). In the functional assay, **13** is a potent inhibitor of $PGD_2$-induced cAMP formation in both washed platelets ($IC_{50}$ = 0.09 nM) and platelet-rich plasma ($IC_{50}$ = 4.0 nM, approximately 4-fold more potent than **12**).

While the *in vitro* profile of **13** attracted our interest, the pharmacokinetic profile of this antagonist remained a potential concern. Gratifyingly, as is evident from the data in Table 3, **13** displays an excellent pharmacokinetic profile in rats with good oral bioavailability ($F$ = 79%) and half-life ($t_{1/2}$ = 7 h) and a low clearance rate (2.4 $mL \cdot min^{-1} \cdot kg^{-1}$). A rat bile duct cannulation study with **13** revealed that low levels of parent drug was present in the biliary fluid ($C_{max}$ = 103 $\mu$M) similar to the other fluoro analogs and in contrast to 7-methylsulfone antagonists **6** or **7**. It thus appears that while the 7-methylsulfonyl antagonists suffer from extensive biliary excretion in rats, the same is not true for the 5-methylsulfone analog **13**. Antagonist **13** also displays excellent pharmacokinetic profiles in other species (mouse, dog, and cynomolgus monkey), and thus the improved rat PK profile of **13** relative to antagonist **6** translated to other species. The behavior of **13** in the *in vitro* rat hepatocyte assay is also worth noting. In this assay, the percent parent remaining from **13** (32%) was similar to the other two fluoro analogs **11** and **12**.

**Covalent Protein Labeling.** Bioactivation of xenobiotics *in vivo* can result in the formation of reactive intermediates resulting in covalent protein adduct formation.[25] This bioactivation−protein modification process has been associated with organ toxicity in both preclinical species and humans. There is also the potential concern that the resulting modified proteins can behave as haptens and induce an unwanted immune response. Our in-house strategy to address the potential liabilities associated with the formation of reactive intermediates has been to incorporate covalent protein labeling studies early in the lead optimization phase of drug discovery. A target of 50 pmol equiv/mg of protein binding is viewed as a low propensity for covalent protein modification.[25]

Up to this point, we have seen how the indole substituents can significantly affect the pharmacokinetic and receptor selectivity profiles of these DP antagonists. Of equal importance, we have observed during the course of our studies that the benzenoid substituents can also affect the level of metabolically activated covalent protein binding. A number of radiolabeled DP antagonists were synthesized[26] (Figure 3) and incubated in rat and human microsomes and hepatocytes for 1 h, and the extent of covalent binding was then evaluated.[27] The results of these experiments are summarized in Table 6. An interesting

**Table 6.** *In vitro* Covalent Protein Binding (pmol equiv/mg of protein per h)[a]

| compd | rat microsomes[b] (+NADPH) | rat hepatocytes[c] | human microsomes[b] (+NADPH) | human hepatocytes[c] |
|---|---|---|---|---|
| **6** | 23 ± 2.1 | 8 ± 0.4 | 18 ± 0.8 | 5 ± 0.5 |
| **7** | 13 ± 4.5 | 9 ± 4.3 | 9 ± 0.4 | <5 ± 0.4 |
| **11** | 460 ± 7.5 | 74 ± 49[d] | 33 ± 1.3 | 33 ± 7.0[d] |
| **12** | 290 ± 50[e] | 45 ± 19[d] | 46 ± 3.3[e] | 16 ± 4.3[d] |
| **13** | 33 ± 0.5 | 38 ± 0.4 | 16 ± 0.5 | 15 ± 1.4 |

[a] Unless indicated otherwise, each value is a mean of triplicate tests from one experiment. [b] Microsomal incubations: 1 mg/mL liver microsomes; 1 mM NADPH; 10 $\mu$M compound (1 $\mu$Ci/mL); 1 h incubation at 37 °C; 125 mM phosphate buffer, pH 7.4. No covalent labeling was observed in the absence of NADPH. [c] Hepatocyte incubations: 0.25 mL of $1 \times 10^6$ cells/mL; preincubation of 20 min at 37 °C under 95/5 $O_2/CO_2$; 10 $\mu$M of test compound (1 $\mu$Ci/mL); 2 h incubation at 37 °C under 95/5 $O_2/CO_2$; 125 mM phosphate buffer, pH 7.4. No covalent labeling was observed in the absence of NADPH. [d] Values shown are means from two separate experiments, each performed in triplicate. [e] Values shown are means from three separate experiments, each performed in triplicate.

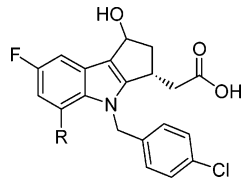


**18**

**Figure 4.** Hydroxyl metabolite of antagonists **11**−**13**.

trend emerges from these *in vitro* protein binding studies. First, for **6** and **7**, both of these antagonists displayed low levels of covalent protein binding in both the rat and human microsomal incubation systems. This low level of protein binding is consistent, in part, with their metabolic stability in the *in vitro* rat hepatocyte assay (Table 3). In contrast, with the fluoro analogs **11** and **12**, high levels of protein binding were observed in the rat microsomal assay (460 and 290 pmol equiv/mg of protein per hour, respectively). The extent of protein binding with these antagonists was lower in the rat hepatocyte assay, and only moderate protein binding was observed in the human incubation systems. With **13**, reduced levels of protein binding were seen in both the rat and human incubation systems relative to **11** and **12** with modest levels of binding in the rat microsomal and hepatocyte systems and low levels in the human incubation systems.

At this point, it is worth commenting on the protein covalent labeling with respect to the corresponding *in vitro* metabolism data presented in Table 4. Antagonist **6** displayed low levels of metabolism in rat hepatocytes and was mainly converted to its corresponding acylglucuronide, along with low levels of a monohydroxylation product. Antagonist **7** exhibited undetectable levels of *in vitro* metabolism in rat hepatocytes. Both of these antagonists display low levels of covalent protein labeling as discussed above. By contrast, the fluoro analogs **11**−**13** are metabolized to a greater extent in vitro (Table 4) with hydroxylation and glucuronidation again being the major pathways. The major site of hydroxylation for these antagonists was assigned to be at carbon 1 (see Figure 1 for numbering scheme) to give the corresponding alcohol **18** (Figure 4) based on LC/MS and NMR studies. For antagonists **11** and **12**, the higher levels of covalent protein labeling, relative to **6** and **7**, correlate with the increased level of *in vitro* metabolism. We have tentatively assigned the structure of the reactive intermediate leading to covalent protein labeling as the iminium cation **19** (Figure 5). Interestingly, while antagonist **13** is metabolized to a similar

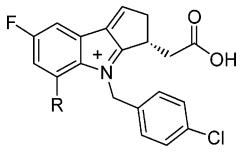


**19**

**Figure 5.** Proposed structure of reactive intermediate.

extent as the other two fluoro analogs **11** and **12**, with glucuronidation and hydroxylation being the major pathways, it differs from these two antagonists in two respects. First, the extent of covalent labeling is significantly lower in both the microsomal and hepatocyte systems. We speculate that the powerful electron-withdrawing methylsulfone substituent present in **13** serves to destabilize the iminium cation **19** and thus inhibit its formation, thereby decreasing the extent of protein covalent labeling. Second, the extent of protein covalent labeling was found to be similar in the microsomal and hepatocyte systems. For antagonists **11** and **12**, the extent of labeling was significantly higher in the rat microsomal incubation than in hepatocytes. One of the major differences between microsomal and hepatocyte systems is that the later possesses naturally occurring trapping agents, such as glutathione, that serve to intercept reactive intermediates. Thus, the decreased protein labeling in rat hepatocyte relative to microsomes for antagonists **11** and **12** is likely the result of the interception of any formed reactive intermediate. The observation that antagonist **13** displays comparable labeling in microsomes as hepatocytes supports the hypothesis that the methylsulfone is preventing the formation of reactive intermediates such as the iminium cation **19**. Thus, the introduction of a methylsulfone at the 5-position of the indole core served two important functions: it improved the DP potency in the functional PRP assay and decreased the propensity for covalent protein labeling.

**Prostanoid Receptor Selectivity.** It is worth commenting further on the DP versus TP selectivities of the above DP antagonists as measured by the receptor binding assay versus the functional assay. This data is summarized in Table 7 and serves to illustrate further the difference between the 7-methylsulfone and 7-fluoro series. For the 7-methylsulfone antagonists **6** and **7**, the TP selectivities measured in the binding assay were found to be consistent with the selectivities observed in the functional assay (Table 7). This is not the case for the 7-fluoro DP antagonists. In all three cases, the TP selectivities of these antagonists were lower in the competition receptor binding assay than in the functional assay. In particular, the TP selectivity of **13** is only 5.2-fold in the binding assay and is 192-fold in the functional assay. Thromboxane ($TxA_2$) acting through the TP receptor is known to induce platelet aggregation; thus inhibition of the TP receptor may result in an inhibition of $TxA_2$-mediated platelet aggregation. In order to determine the true TP selectivity of **13**, a number of experiments were initiated in an effort to resolve this apparent discrepancy. The lower limit of sensitivity in the competition receptor binding assays is approximately 0.5 nM; thus selectivity ratios determined with this assay may be underestimating the selectivity of antagonist **13**. To circumvent this limitation, the dissociation constants ($K_d$) for **13** from the DP and TP receptors were measured. From these experiments, the $K_d$'s for **13** from the DP and TP receptors were determined to be 0.03 and 10.9 nM, respectively. The TP selectivity for **13**, as determined from the dissociation data, is now 360-fold, which is in agreement with the selectivity measured in the functional assay. Thus, the apparent discrepancy in DP versus TP selectivity of **13** as measured from the

**Table 7.** DP Receptor Selectivities of DP Antagonists[a]

| | receptor binding | | | functional | | |
|---|---|---|---|---|---|---|
| compd | DP $K_i$ (nM) | TP $K_i$ (nM) | selectivity (DP vs TP) | DP PRP $IC_{50}$[b] (nM) | TP PRP $IC_{50}$[c] (nM) | selectivity (DP vs TP) |
| **6** | 2.6 ± 0.7 | 1200 ± 470 | 460 | 7.9 ± 2.8 | 8400 ± 4700 | 1100 |
| **7** | 1.8 ± 0.7 | 7100 ± 820 | 3900 | 8.6 ± 4.3 | 43000 ± 16000 | 5100 |
| **11** | 1.5 ± 0.57 | 0.84 ± 0.19 | 0.56 | 23 ± 9.5 | 80 ± 60 | 3.5 |
| **12** | 1.1 ± 0.22 | 14 ± 2.7 | 13 | 15 ± 0.41 | 1400 ± 1000 | 93 |
| **13** | 0.57 ± 0.17 | 2.95 ± 0.46 | 5.2 | 4.0 ± 0.9 | 770 ± 490 | 192 |

[a] Values are means from at least three experiments. [b] DP PRP assay: inhibition of the accumulation of cAMP in platelet-rich plasma challenged with $PGD_2$. [c] TP PRP assay: the inhibition of U44619-induced platelet aggregation in platelet-rich plasma.

**Table 8.** Effect of **13** in Inhibiting Nasal Airway Resistance Induced by Intranasal Instillation of $PGD_2$ in Conscious Sheep[a]

| dose (mg/kg) | inhibition of nasal airway resistance (%) | plasma levels of antagonist **13** (nM)[b,c] |
|---|---|---|
| 0.03 | 26 ± 10.7 | 91 (range 37−152 nM) |
| 0.1 | 99 ± 0.7 | 670 (range 103−1260 nM) |

[a] Values are the means of at least three experiments. [b] Plasma levels determined at time of intranasal $PGD_2$ challenge. [c] Sheep DP PRP $IC_{50}$ = 1.4 ± 0.2 nM ($n$ = 3).

competition binding assay versus the functional assay was likely the result of the limitation in the dynamic range of the DP receptor binding assay. The DP and TP binding affinities for the enantiomer of **13** (**20**) were found to be 9.6 and 1050 nM respectively. Thus while **20** remains a relatively potent DP antagonist, it is approximately 320-fold less potent than **13**.[28] In addition, antagonist **13** is also selective for the $CRTH_2$ receptor (a recently identified second $PGD_2$ receptor[29]), displaying a $K_i$ of 745 ± 319 nM.

***In vivo* Efficacy of 13.** The potent DP antagonist **13** was evaluated in a conscious sheep model of $PGD_2$-induced congestion. The sheep model was selected as an in vivo model to evaluate the DP antagonists since sheep have been extensively used to study lower-airway disorders and this model has recently been adapted to examine upper-airway disorders such as allergic rhinitis.[30] The potency ($IC_{50}$) of **13** on the sheep DP receptor in the platelet-rich plasma (PRP) assay was measured to be 1.4 ± 0.2 nM, comparable to the potency on the human receptor. Having established that antagonist **13** is active on the sheep DP receptor, it was then evaluated in the sheep allergic rhinitis model. Thus, antagonist **13** was administered intravenously, and 30 min later the sheep were challenged with an intranasal instillation of $PGD_2$ and changes in nasal airflow resistance were measured by rhinomanometry. As summarized in Table 8, while only a modest level of inhibition (26%) was observed at a dose of 0.03 mg/kg, a dose of 0.1 mg/kg of antagonist **13** provided complete (99%) blockade of the $PGD_2$ induced nasal congestion. The plasma levels of antagonist **13** at the time of $PGD_2$ challenge are provided in Table 8 and are well above the PRP $IC_{50}$ value for antagonist **13**. It is worth noting that these plasma drug levels may not reflect the drug levels at the site of action, that is, the nasal vasculature. Thus, in addition to being a potent DP receptor antagonist *in vitro*, **13** is also effective in a sheep model of nasal congestion.

## Conclusion

In summary, we have presented the discovery of **13**[31], a potent and selective DP receptor antagonist. This antagonist has a high affinity for the DP receptor with a competition binding affinity constant ($K_i$) of 0.57 nM and a dissociation constant ($K_d$) of 0.03 nM. Antagonist **13** is 192-fold selective for the thromboxane receptor based on a ratio of $K_d$ values at the DP and TP receptors. Antagonist **13** is also potent in a DP functional assay where it inhibits the $PGD_2$-induced cAMP production in platelet-rich plasma with an $IC_{50}$ of 4.0 nM. Antagonist **13** was also shown to display an excellent rat pharmacokinetic profile. Antagonist **13** was also efficacious in a sheep model of allergic rhinitis.

As part of the medicinal chemistry effort leading to the discovery of **13**, the initial lead antagonists **6** and **7** were shown to display poor pharmacokinetic profiles. Rat bile duct cannulation studies demonstrated that the rapid clearance of these antagonists was likely a result of active hepatic excretion of parent drug into the biliary fluid. The pharmacokinetic issues with the 7-methylsulfonyl antagonists **6** and **7** were effectively circumvented by replacing the methylsulfone substituent with a fluorine atom. Reintroduction of the methylsulfone at the 5-position of the indole led to the discovery of **13**. Several key observations noted during the discovery of **13** were that apparently subtle changes in the substitution pattern of a molecule can result in significant pharmacokinetic effects. Also, while *in vitro* metabolic studies are invaluable in drug discovery, it is equally important to augment this data with *in vivo* pharmacokinetic/metabolism studies to help understand the clearance mechanism of a drug candidate. Thus, based on these observations, the strategy we employed to circumvent a biliary excretion/poor pharmacokinetic issue with our lead DP antagonist was to introduce modifications at different regions of the molecule and examine the effect of these changes on the PK profile directly. In doing so, we were able to identify analogs with significantly reduced biliary excretion. In addition, it was observed that the extent of covalent protein binding can be attenuated, at least in the context of the current indole series, by the introduction of a powerful electron-withdrawing substituent such as a methylsulfone on the indole core. The $PGD_2$ receptor antagonist **13** has been studied in a clinical model of allergic rhinitis, and the results of these trials will be reported in due course.

## Experimental Procedures

**General Experimental Methods.** Melting points are uncorrected. NMR spectra were recorded in the indicated solvent with the protonated form as the internal standard for $^1H$ (400 MHz or 500 MHz) and for $^{13}C$ (100 MHz or 125 MHz). TLC analyses were performed on Merck Kieselgel 60 F254 plates. All air-sensitive reactions carried out under a nitrogen atmosphere. Column chromatography was performed with silica gel 230−400 mesh. Elemental analyses were performed by Prevalere Life Sciences, Inc., Whitesboro, NY. The LC/MS and LC/MS/MS studies were performed using a PE Sciex API 2000 instrument. The HPLC-UV analyses were performed using a Waters 2690 HPLC system equipped with a photodiode array detector. For the rat pharmacokinetic and bile duct cannulation studies, all aspects of housing, care, and use of the animals were in accordance with the guidelines of the Canadian Council on Animal Care and the "Guide to the Care and Use of Experimental Animals".

**Pharmacokinetic Studies.** Sprague−Dawley rats were fasted overnight and prior to dosing with test compound given either by

oral gavage or intravenously. At various time points, blood samples were collected by tail bleed, and this blood was centrifuged to furnish plasma samples. The plasma was stored at −10 °C until time of analysis. At this time, plasma proteins were precipitated by treating 100 μL of the plasma samples with 100 μL of acetonitrile. The samples thus obtained were vortexed and centrifuged. The resulting supernatants were transferred into sample vials and subsequently analyzed by LC/MS/MS. Reference standard samples for each test compound were prepared as described above using plasma derived from the blood of untreated rats and subsequently spiked with known concentrations of test compound typically ranging from 0.01 to 10 μg/mL.

**Bile Duct Cannulation Studies.** The bile duct cannulation studies were performed as described in ref 23. Male Sprague−Dawley rats were obtained from Charles River Laboratories (St. Constant, Quebec, Canada) and were acclimatized for at least 48 h before use. The rats (∼350 g) were anesthetized with ketamine (75 mg/kg) and xylazine (5 mg/kg) throughout the duct cannulation procedure. Blank bile fluid was collected for a period of 30 min prior to drug treatment. The test compounds were then administered intravenously in the jugular vein at a dose of 5 mg/kg in either 5% dextrose or 60% PEG 200 with a dose volume of 1 mL/kg. Bile samples were then collected in 30 min intervals and kept at −10 °C before analysis. The bile samples were processed as follows: 100 μL of bile fluid was treated with 100 μL of $CH_3CN$ and 200 μL of water. The samples were then vortexed and centrifuged. The resulting supernatants were transferred into sample vials and analyzed by LC-UV. Reference samples were prepared using blank bile fluid following the procedure described above and spiking with known concentrations of test compound.

**Receptor Binding and DP and TP Functional Assays.** The receptor binding assays were performed as described in ref 19. The DP functional assays were performed as follows: Blood was collected from normal human volunteers, free from medication for two weeks, by venous puncture. The blood was collected in Vacutainers without additive and transferred immediately into 50 mL tubes containing 10% (v/v) citrate buffer (65 mM citric acid, 85 mM sodium citrate, 2% (v/v) glucose) and then mixed by inversion. Platelet-rich plasma (PRP) was prepared by centrifugation at 150 × *g* for 15 min. The PRP was removed and transferred into a clean tube. Half of the resulting PRP fraction from each donor was used to prepare washed platelets (WP). Citrate buffer (30% v/v) and 50% v/v of 25 mM HEPES, pH 7.4, Hanks' balanced salt solution (HBSS) without $Ca^{2+}$ or $Mg^{2+}$ were added to PRP, and the mixture was centrifuged for 10 min at 800 × *g*. The cell pellet was resuspended in 1/10th of the original blood volume in 25 mM HEPES, pH 7.4, HBSS with $Ca^{2+}$ and $Mg^{2+}$ containing 10% (v/v) citrate buffer, centrifuged, and resuspended as above. The cells were recentrifuged a third time as above and resuspended in 5 mL of 25 mM HEPES, pH 7.4, HBSS without $Ca^{2+}$ or $Mg^{2+}$. Platelet cell counting was determined in a Beckman Z-2 Coulter counter. Platelet cell counts in the PRP and WP assays were adjusted to $2.5 \times 10^8$ cells/mL using 25 mM HEPES, HSBB without $Ca^{2+}$ or $Mg^{2+}$. The WP and PRP assays were conducted as follows: isobutylmethylxanthine (IBMX; 2 mM final concentration) was added to human WP or PRP to prevent degradation of cAMP. Samples (100 μL) of either human WP or PRP were then preincubated (10 min at 37 °C) with increasing concentrations of test compound in DMSO [1% (v/v) final in assay, kept constant in all samples]. Samples were then challenged with $PGD_2$ (300 nM final) added in DMSO (kept constant at 1% (v/v) throughout) and incubated for an additional 2 min at 37 °C. $PGD_2$ was not metabolized during the 2 min incubation period as determined by HPLC-MS analysis. The reaction was then terminated by the addition of 200 μL of ethanol to disrupt the cells and extract the cAMP. The samples were mixed thoroughly and centrifuged at 1400 × *g* for 10 min at 4 °C. Supernatant aliquots (100 μL) were removed, and the ethanol was removed by evaporation. cAMP was measured by [$^{125}$I]-cAMP scintillation proximity assay (SPA) (RPA556, Amersham) according to the manufacturer's instructions following reconstitution of the samples in SPA buffer. cAMP accumulation assays were conducted using matched WP and PRP from individual donors.

The TP functional assays were performed as follows: Test compounds were assessed for their ability to inhibit platelet aggregation in human platelet-rich plasma (PRP) using aggregometry. Citrated blood was collected from donors who were medication free for at least two weeks. After gentle mixing of the blood and citrate, samples were centrifuged at 150 × *g* for 15 min at rt and the upper phase was removed in order to obtain PRP. Platelet poor plasma (PPP) was prepared by centrifugation of the lower phase after PRP removal at 2000 × *g* for 10 min at rt. Platelet concentrations were adjusted to $2.5 \times 10^8$ platelet/mL using PPP. The adjusted PRP (250 μL) was stirred in a cuvette at 37 °C for 3 min, and 25 μL of the test compound diluted in buffer [0.9% (w/v) or 0.15 M NaCl containing 0.25% (w/v) BSA] or vehicle (buffer), as control, was added to 250 μL of stirring platelets for a 10 min preincubation period. Agonist (20 μL, 1.36 μM U46619,[32] final concentration, diluted buffer) was then added to the stirring PRP mixture to induce aggregation, and the incubation continued for 5 min. Maximium aggregation was determined at approximately 5 min. The maximum extent of aggregation achieved in the presence of U46619 was set to 100%.

**Ethyl [7-(Methylsulphonyl)-1,2,3,4-tetrahydrocyclopenta[*b*]-indol-3-yl]acetate (2).** To a vigorously stirred solution 4-(methylsulfonyl)-phenylamine (100 g, 584 mmol) dissolved in EtOH (5.5 L) at 50 °C was added a mixture of iodine (49.3 g, 194 mmol) and silver sulfate (110 g, 353 mmol) in EtOH (1 L). The addition of iodine and silver sulfate was repeated twice more after 1 and 2 h of stirring, and the resulting mixture was allowed to stir overnight. The hot solution was then filtered through Celite, and the solvent was removed under vacuum. The residue was triturated with warm (50 °C) EtOH (1 L) for 45 min and then cooled to 0 °C. The resulting product was filtered and collected to provide 2-iodo-4-(methylsulfonyl)phenylamine as a brown solid (140 g, 80%). $^1$H NMR (acetone-$d_6$): δ 8.08 (d, $J$ = 2.0 Hz, 1H), 7.63 (dd, $J$ = 8.5 and 2.0 Hz, 1H), 6.93 (d, $J$ = 8.5 Hz, 1H), 5.78 (br s, 2H), 3.03 (s, 3H). $^{13}$C NMR (acetone-$d_6$): δ 153.6, 139.3, 130.6, 129.7, 114.0, 81.0, 44.8. Mp 201−201 °C. MS (+APCI) *m*/*z* 298.2 $(M + H)^+$. Anal. ($C_7H_8NO_2SI$) C, H, N.

A solution of 2-iodo-4-(methylsulfonyl)phenylamine (150 g, 503 mmol) and PPTS (4.8 g, 19.1 mmol) in DMF (3.0 L) was degassed and kept under a $N_2$ atmosphere, and tetraethoxysilane (135 g, 640 mmol) and ethyl 2-(2-oxocyclopentyl)acetate (129 g, 758 mmol) were then added. The final mixture was heated to 130−140 °C and stirred for 6 h. Then, DMF (300 mL) was added, and the solution was degassed before Hunig's base (270 mL, 1550 mmol) followed by $Pd(OAc)_2$ (3.4 g, 15.1 mmol) were added successively. The solution was heated to 120 °C for 2 h and then cooled to rt. At this time, a 1 N HCl (300 mL) solution and isopropyl acetate (200 mL) were added, and the resulting mixture was filtered through Celite. The phases were separated, and the acidic phase was extracted twice with isopropyl acetate (200 mL). The organic layers were combined, washed with brine, dried over anhydrous $Na_2SO_4$, filtered through Celite, and concentrated. The crude material was further purified by flash chromatography, eluting with 50% EtOAc in hexanes, to provide ethyl [7-(methylsulphonyl)-1,2,3,4-tetrahydrocyclopenta[*b*]indol-3-yl]acetate as a yellow solid (63 g, 39%). $^1$H NMR (acetone-$d_6$): δ 10.23 (br s, 1H), 7.98 (s, 1H), 7.50−7.50 (m, 2H), 4.14 (q, $J$ = 7.1 Hz, 2H), 3.70−3.58 (m, 1H), 3.04 (s, 3H), 2.90−2.65 (m, 5H), 2.20−2.10 (m, 1H), 1.22 (t, $J$ = 7.1 Hz, 3H). MS (+APCI) *m*/*z* 322.2 $(M + H)^+$.

**[5-Bromo-4-(4-chlorobenzyl)-7-(methylsulfonyl)-1,2,3,4-tetrahydrocyclopenta[*b*]indol-3-yl]acetic Acid (3).** To a solution of **2** (61.5 g, 192 mmol) in THF (550 mL) at rt, MeOH (275 mL), followed by 2 N NaOH (275 mL, 550 mmol), was added. The reaction was heated to 60 °C for 15 min, cooled to rt, and then poured into a separatory funnel containing EtOAc/1 N HCl. The phases were separated, and the acidic phase was extracted twice with EtOAc. The organic layers were combined, washed with brine, dried over anhydrous $Na_2SO_4$, and evaporated to dryness. The crude solid was triturated in EtOAc/hexanes to give [7-(methylsulfonyl)-

1,2,3,4-tetrahydrocyclopenta[*b*]indol-3-yl]acetic acid as a faint brown solid, 56.0 g (quantitative yield). $^1$H NMR (acetone-$d_6$): $\delta$ 10.86 (br s, 1H), 10.25 (br s, 1H), 7.98 (s, 1H), 7.58 (m, 2H), 3.62 (m, 1H), 3.04 (s, 3H), 2.89−2.68 (m, 5H), 2.21 (m, 1H); $^{13}$C NMR (DMSO-$d_6$): $\delta$ 173.7, 149.6, 143.6, 131.4, 123.6, 119.3, 118.6, 118.5, 112.8, 45.1, 39.4, 36.0, 35.5, 23.4. Mp 208 °C. MS (+APCI) *m*/*z* 294.0 (M + H)$^+$. Anal. ($C_{14}H_{15}NO_4S$) C, H, N.

Pyridinium tribromide (154 g, 481.5 mmol) was added to a solution of 2-[7-(methyl-sulfonyl)-1,2,3-trihydrocyclopenta[2,3-*b*]-indol-3-yl]acetic acid (50.8 g, 173.1 mmol) in pyridine (345 mL) at −25 to −30 °C; the solution was warmed to 0 °C for 15 min and then to rt for 30 min. At this time, a 1:1 solution of THF/ether (1.25 L) and a 1:1 brine/6 N HCl solution (2.5 L) were added, the phases were separated, the aqueous layer was washed with 1:1 THF/ether, and the combined organic layers were dried with $Na_2SO_4$. The organic phase was cooled to 10 °C, and acetic acid (50.5 mL) was added followed by a slow addition of zinc dust (70.2 g, 1074 mmol) while maintaining the temperature below 15 °C. The reaction mixture was then stirred for 1 h at rt. To this mixture, 1 N HCl (3 L) and EtOAc (1.25 L) were added; the phases were separated, and the aqueous layer was extracted with EtOAc (2 L). The combined organic layers were dried with $Na_2SO_4$, and the solvent was removed under vacuum. The resulting brownish powder was stirred with a 20% EtOAc/hexanes solution (1000 mL) to furnish [5-bromo-4-(4-chlorobenzyl)-7-(methylsulfonyl)-1,2,3,4-tetrahydrocyclopenta[*b*]indol-3-yl]acetic acid (52 g, 81%). $^1$H NMR (acetone-$d_6$): $\delta$ 11.05 (br s, 1H), 10.37 (br s, 1H), 8.00 (s, 1H), 7.76 (d, $J$ = 1.2 Hz, 1H), 3.66 (m, 1H), 3.13 (s, 3H), 3.00−2.75 (m, 4H), 2.62 (dd, $J$ = 16.5 and 8.2 Hz, 1H,), 2.27 (m, 1H). $^{13}$C NMR (DMSO-$d_6$): $\delta$ 173.3, 150.2, 140.7, 132.5, 124.5, 120.4, 120.3, 117.7, 104.3, 44.3, 38.5, 35.4, 35.2, 23.1. MS (−APCI) *m*/*z* 372.2, 370.2 (M − H)$^-$. Anal. ($C_{14}H_{14}BrNO_4S$) C, H, N.

**Methyl [5-Bromo-4-(4-chlorobenzyl)-7-(methylsulfonyl)-1,2,3,4-tetrahydrocyclopenta[*b*]indol-3-yl]acetate (4).** Acid **3** (12.0 g, 24.1 mmol) in THF (450 mL) was esterified with an ether solution of $CH_2N_2$. After removal of the solvents, methyl [5-bromo-7-(methylsulfonyl)-1,2,3,4-tetrahydrocyclopenta[*b*]indol-3-yl]acetate was obtained as a pale brown solid (12.5 g, quantitative). $^1$H NMR (acetone-$d_6$): $\delta$ 10.41 (br s, 1H), 8.03 (d, $J$ = 1.0 Hz, 1H), 7.79 (d, $J$ = 1.5 Hz, 1H), 3.71 (s, 3H), 3.70−3.68 (m, 1H), 3.27 (s, 3H), 3.14−2.92 (m, 2H), 2.86−2.82 (m, 2H), 2.64 (dd, $J$ = 16.2 and 8.3 Hz, 1H), 2.29−2.23 (m, 1H). $^{13}$C NMR (acetone-$d_6$): $\delta$ 172.7, 149.7, 141.1, 133.5, 125.0, 121.6, 121.0, 118.2, 104.3, 51.1, 44.3, 38.3, 35.52, 35.48, 23.1. Mp 128−130 °C. MS (−APCI) *m*/*z* 386.0, 384.0 (M − H)$^-$; Anal. ($C_{15}H_{16}BrNO_4S$) C, H, N.

To a solution of the above ester (8.8 g, 22.8 mmol) in DMF (90 mL) at −78 °C was added NaH (60% in oil, 790 mg, 19.8 mmol). The resulting suspension was stirred for 20 min at 0 °C, cooled again to −40 to − 50 °C and treated with 4-chloro-benzyl bromide (5.60 g, 27.3 mmol). After 5 min, the temperature was warmed to 0 °C, and the solution was stirred for 20 min. At this time, the reaction mixture was quenched by the addition of AcOH (2.6 mL), and this mixture was poured into a separatory funnel containing 1 N HCl/EtOAc. The layers were separated, and the organic layer was washed with brine, dried over anhydrous $Na_2SO_4$, and concentrated. The crude material was further purified by flash chromatography eluting with 10% EtOAc in toluene to provide methyl [5-bromo-4-(4-chlorobenzyl)-7-(methylsulfonyl)-1,2,3,4-tetrahydrocyclopenta[*b*]indol-3-yl]acetate as a white solid (10.1 g, 89%). $^1$H NMR (acetone-$d_6$): $\delta$ 8.06 (d, $J$ = 1.6 Hz, 1H), 7.76 (d, $J$ = 1.6 Hz, 1H), 7.36 (d, $J$ = 8.5 Hz, 2H), 6.98 (d, $J$ = 8.4 Hz, 2H), 6.00 (d, $J_{AB}$ = 17.8 Hz, 1H), 5.89 (d, $J_{AB}$ = 17.8 Hz, 1H), 3.71−3.67 (m, 1H), 3.59 (s, 3H), 3.17 (s, 3H), 3.05−2.97 (m, 1H), 2.92−2.80 (m, 2H), 2.69 (dd, $J$ = 16.2 and 3.8 Hz, 1H), 2.48 (dd, $J$ = 16.2 and 9.8 Hz, 1H), 2.35−2.28 (m, 1H). $^{13}$C NMR (acetone-$d_6$): $\delta$ 171.6, 152.3, 138.8, 138.2, 133.8, 132.5, 128.7, 127.2, 126.9, 123.9, 121.3, 118.5, 103.4, 50.9, 48.6, 44.0, 37.9, 35.5, 35.3, 22.5. Mp 108−111 °C. MS (+APCI) *m*/*z* 512.0, 510.0 (M + H)$^+$.

**[5-Acetyl-4-(4-chlorobenzyl)-7-(methylsulfonyl)-1,2,3,4-tetrahydrocyclopenta[*b*]indol-3-yl]acetic Acid (5).** To a solution of **4** (10.0 g, 29.9 mmol) in DMF (100 mL) was added 1-ethoxyvinyltributyltin (10.8 g, 29.8 mmol). The resulting mixture was degassed by bubbling $N_2$ through the solution for several minutes. In a separate flask was placed $Pd_2(dba)_3$ (1.04 g, 1.14 mmol) and $Ph_3As$ (2.8 g, 9.2 mmol) along with DMF (100 mL), and this mixture was sonicated for 10 min to provide a fine suspension. The resulting catalyst mixture was then introduced into the above reaction flask, which was heated at 80 °C for 3 h. After the reaction was allowed to cool to rt, a 3 N HCl solution (100 mL) was added to the reaction flask, and the mixture was allowed to stir until TLC analysis indicated the consumption of the vinyl ether adduct. The reaction mixture was diluted with water, extracted with ethyl acetate, dried over anhydrous $Na_2SO_4$, and concentrated. The resulting material was further purified by flash chromatography, eluting with 15% ethyl acetate in hexanes followed by recrystallization from 20% ethyl acetate in hexane, to provide methyl [5-acetyl-4-(4-chlorobenzyl)-7-(methylsulfonyl)-1,2,3,4-tetrahydrocyclopenta[*b*]indol-3-yl]acetate as a white solid (6.3 g, 66%). $^1$H NMR ($CDCl_3$): $\delta$ 8.22 (d, $J$ = 1.8 Hz, 1H), 7.89 (d, $J$ = 1.8 Hz, 1H), 7.31−7.28 (m, 2H), 6.77−6.74 (m, 2H), 5.48 (s, 2H), 3.83−3.79 (m, 1H), 3.62 (s, 3H), 3.15 (s, 3H), 3.09−3.00 (m, 1H), 2.96−2.90 (m, 2H), 2.88−2.79 (m, 1H), 2.60 (dd, $J$ = 16.0 and 9.7 Hz, 1H), 2.41−2.35 (m, 1H), 2.20 (s, 3H). $^{13}$C NMR (acetone-$d_6$): $\delta$ 199.3, 171.6, 152.8, 137.5, 136.3, 132.6, 132.0, 128.7, 128.3, 127.4, 126.7, 121.8, 120.6, 119.6, 50.9, 49.8, 44.0, 38.1, 35.6, 35.3, 28.1, 22.6. MS (+APCI) *m*/*z* 476.1, 474.1 (M + H)$^+$.

The above ester (2.08 g, 4.4 mmol) was hydrolyzed following the procedure outlined for compound **3** to yield [5-acetyl-4-(4-chlorobenzyl)-7-(methylsulfonyl)-1,2,3,4-tetrahydrocyclopenta[*b*]indol-3-yl]acetic acid (1.99 g, 99%) as a brownish solid. $^1$H NMR (acetone-$d_6$): $\delta$ 10.76 (br s, 1H), 8.19 (d, $J$ = 1.7 Hz, 1H), 7.87 (d, $J$ = 1.7 Hz, 1H), 7.27 (d, $J$ = 8.5 Hz, 2H), 6.73 (d, $J$ = 8.4 Hz, 2H), 5.48 (s, 2H), 3.79 (m, 1H), 3.12 (s, 3H), 3.05 (m, 1H), 3.00−2.70 (m, 3H), 2.55 (dd, $J$ = 16.2 and 9.9 Hz, 1H), 2.38 (m, 1H), 2.19 (s, 3H). $^{13}$C NMR (acetone-$d_6$): $\delta$ 199.3, 172.3, 153.0, 137.5, 136.4, 132.6, 131.7, 128.7, 128.3, 127.4, 126.7, 121.8, 120.6, 119.6, 49.8, 44.0, 38.1, 35.6, 35.4, 28.1, 22.6. Mp 152−155 °C. MS (−ESI) *m*/*z* 459.8, 457.7 (M − H)$^-$.

**[(3*R*)-5-Acetyl-4-(4-chlorobenzyl)-7-(methylsulfonyl)-1,2,3,4-tetrahydrocyclopenta[*b*]indol-3-yl]acetic Acid (6).** (±)-[5-Acetyl-4-(4-chlorobenzyl)-7-(methylsulfonyl)-1,2,3,4-tetrahydrocyclopenta-[*b*]indol-3-yl]acetic acid (**5**) dissolved in EtOH was resolved using normal phase preparative chiral HPLC [ChiralPak AD column, 50 cm × 5 cm, 20 $\mu$m; mobile phase hexane/2-propanol/acetic acid (70:30:0.4); flow 70−75 mL/min; pressure 280−300 psi; UV 265 nm]. Retention times of the two enantiomers were 38 and 58 min. The title (*R*) isomer (retention time 58 min) was thus obtained with a 96.7% ee. Retention time = 15.3 min [ChiralPak AD column 250 mm × 4.6 mm, hexane/2-propanol/acetic acid (75:25:0.1)]. $[\alpha]_D^{21} = -10.9°$ (*c* 0.45, MeOH). $^1$H NMR (acetone-$d_6$): $\delta$ 10.80 (br s, 1H), 8.22 (d, $J$ = 1.7 Hz, 1H), 7.89 (d, $J$ = 1.7 Hz, 1H), 7.30 (d, $J$ = 8.5 Hz, 2H), 6.76 (d, $J$ = 8.4 Hz, 2H), 5.50 (s, 2H), 3.83−3.78 (m, 1H), 3.15 (s, 3H), 3.11−3.03 (m, 1H), 2.97−2.90 (m, 2H), 2.85−2.80 (m, 1H), 2.58 (dd, $J$ = 16.1 and 9.9 Hz, 1H), 2.45−2.39 (m, 1H), 2.20 (s, 3H). $^{13}$C NMR (acetone-$d_6$): $\delta$ 199.3, 173.0, 153.0, 137.3, 136.4, 132.6, 131.7, 128.7, 128.3, 127.4, 126.7, 121.8, 120.6, 119.6, 49.8, 44.9, 38.1, 35.6, 35.4, 28.1, 22.6. Mp 219 °C. MS (−APCI) *m*/*z* 460.5, 458.3 (M − H)$^-$. Anal. ($C_{23}H_{22}ClNO_5S$) C, H, N, S.

**[(3*R*)-4-(4-Chlorobenzyl)-5-(1-hydroxyethyl)-7-(methylsulfonyl)-1,2,3,4-tetrahydrocyclopenta[*b*]indol-3-yl]acetic acid (7).** In a dry flask was placed (−)-[(3*R*)-5-acetyl-4-(4-chlorobenzyl)-7-(methylsulfonyl)-1,2,3,4-tetrahydrocyclopenta[*b*]indol-3-yl]acetic acid (350 mg, 0.76 mmol) along with MeOH (30 mL). To this stirred solution was added $NaBH_4$ portion-wise (ca. 50 mg/portion) in 10−15 min intervals until the consumption of ketone was noted by TLC analysis. At this time, the reaction mixture was poured into a separatory funnel containing saturated aqueous $NH_4Cl$ solution (100 mL), a 1 N HCl solution (10 mL), and EtOAc (100 mL). The layers were separated, and the aqueous layer was extracted with EtOAc; the combined organic layers were dried over anhydrous $Na_2SO_4$ and concentrated. The resulting material was purified by chiral

HPLC as follows. The mixture of alcohols dissolved in hot EtOH was resolved using normal phase preparative chiral HPLC [ChiralPak AD column 50 cm × 5 cm, 20 $\mu$m; mobile phase hexane/2-propanol/acetic acid (80:20:0.4); flow 70−75 mL/min; pressure 280−300 psi; UV 245 nm]. Retention times of the two diastereoisomers were 33 and 51 min. The title compound (retention time 33 min) was obtained with >99% de; ee = 99%. Retention time = 6.0 min [ChiralPak AD column 250 mm × 4.6 mm, hexane/2-propanol/acetic acid (75:25:0.2)]. $[\alpha]_D^{21} = +7.6°$ (*c* 1.0, MeOH). $^1$H NMR (acetone-$d_6$): $\delta$ 7.97 (s, 1H), 7.86 (s, 1H), 7.35 (d, $J$ = 8.2 Hz, 2H), 6.90 (d, $J$ = 8.2 Hz, 2H), 5.92 (d, $J_{AB}$ = 18.1 Hz, 1H), 5.68 (d, $J_{AB}$ = 18.1 Hz, 1H), (q, $J$ = 5.19 Hz, 1H), 3.63−3.55 (m, 1H), 3.09 (s, 3H), 3.08−2.91 (m, 1H), 2.89−2.79 (m, 2H), 2.70−2.65 (m, 1H), 2.46−2.34 (m, 2H), 1.49 (d, $J$ = 6.3 Hz, 3H). $^{13}$C NMR (acetone-$d_6$): $\delta$ 173.3, 152.0, 141.1, 139.4, 133.3, 133.2, 132.6, 129.7, 127.8, 126.4, 121.7, 118.8, 117.3, 64.6, 50.3, 45.0, 39.1, 36.5, 36.2, 24.6, 23.5. MS (−APCI) *m*/*z* 462.8, 460.5 $(M - H)^-$. Mp 212 °C. Anal. ($C_{23}H_{24}ClNO_5S$) C, H, N, S.

**Ethyl (7-Fluoro-1,2,3,4-tetrahydrocyclopenta[*b*]indol-3-yl)-acetate (9).** To a mixture of 4-fluoroaniline (36 mL, 380 mmol) in water (1 L) and toluene (30 mL) was added $NaHCO_3$ (50.4 g, 599 mmol) and iodine (75.4 g, 298 mmol) over a period of 30 min. The resulting reaction was then stirred at rt for 30 min. At this time, the reaction was poured into water, and the pH was adjusted to 6−7 with an HCl solution. The aqueous layer was extracted with $Et_2O$ (2×), washed with 5% $Na_2S_2O_3$ solution (2×), and washed with brine. The resulting solution was dried over anhydrous $Na_2SO_4$, filtered over a plug of silica gel, and concentrated. The resulting material was distilled under high vacuum (bp 74−76 °C) to yield 4-fluoro-2-iodoaniline as an orange oil (40.2 g, 57%). This material was immediately used in the next reaction. $^1$H NMR ($CDCl_3$): $\delta$ 7.35 (dd, $J$ = 7.9 and 2.6 Hz, 1H), 6.90−6.85 (m, 1H), 6.68−6.65 (m, 1H), 3.92 (br s, 2H).

Following the procedure outlined for compound **2**, the 4-fluoro-2-iodoaniline (10.0 g, 42.2 mmol) was treated with ethyl-2-(2-oxocyclopentyl)acetate (6.57 g, 38.6 mmol) to yield ethyl (7-fluoro-1,2,3,4-tetrahydrocyclopenta[*b*]indol-3-yl)acetate as a yellow solid (5.3 g, 53%). $^1$H NMR (acetone-$d_6$): $\delta$ 9.76 (br s, 1H), 7.34 (dd, $J$ = 8.8 and 4.6 Hz, 1H), 7.03 (d, $J$ = 9.9 Hz, 1H), 6.78 (td, $J$ = 9.5 and 2.3 Hz, 1H), 4.14 (q, $J$ = 7.1 Hz, 2H), 3.58−3.54 (m, 1H), 2.85−2.55 (m, 5H), 2.16−2.12 (m, 1H), 1.22 (t, $J$ = 7.1 Hz, 3H).

**Alternative Indole Synthesis.** To a flask equipped with a Dean−Stark apparatus was added 2-bromo-4-fluoroaniline (500 g, 2.63 mmol), toluene (5 L), ethyl 2-(2-oxocyclopentyl)acetate (448 g, 2.63 mmol), and *p*-TsOH·$H_2O$ (3.3 g, 17.3 mmol). The resulting mixture was stirred with the aid of a mechanical stirrer and heated to reflux for 20 h. At this time, the reaction was cooled to rt and concentrated. The resulting material was treated with DMF (5 L), KOAc (774 g, 7.89 mmol), $^n$$Bu_4NCl$ (775 g, 2.63 mmol), and $Pd(OAc)_2$ (17.7 g, 78.9 mmol), evacuated under house vacuum, and flushed with nitrogen three times. The mixture was then heated to 80 °C for 1 h. The resulting reaction was poured slowly into a mixture of $H_2O$ (20 L) and EtOAc (10 L) and stirred; the layers were separated, and the organic layer was washed with $H_2O$ (2 × 10 L), dried over anhydrous $Na_2SO_4$, and concentrated. The resulting oil was purified by flash chromatography, eluting with 5−10% EtOAc/hexane. Concentration of the chromatography fractions that contained the desired product provided a solid material that was subsequently stirred with hexanes and filtered, and the residue was washed with hexanes to yield 210 g of a white solid. The hexane washings were combined, washed with 1 N HCl, dried over anhydrous $Na_2SO_4$, concentrated, and heated to 75 °C under high vacuum. The resulting solid was purified by flash chromatography as described above to provide an additional 42.0 g of a white solid. The desired indole (ethyl (7-fluoro-1,2,3,4-tetrahydrocyclopenta[*b*]indol-3-yl)acetate) was obtained in a total yield of 252 g (37%) as a white solid.

**[5-Bromo-4-(4-chlorobenzyl)-7-fluoro-1,2,3,4-tetrahydrocyclopenta[*b*]indol-3-yl]acetic Acid (10).** Following the procedure described for **3**, hydrolysis of ester **9** (200 g, 760 mmol) yielded the corresponding acid as a brown oil that was used as such in the next step (165 g, 92%). $^1$H NMR (acetone-$d_6$): $\delta$ 10.50 (br s, 1H), 9.75 (br s, 1H), 7.34 (dd, $J$ = 8.8 and 4.6 Hz, 1H), 7.04 (dd, $J$ = 9.9 and 2.4 Hz, 1H), 6.79 (m, 1H), 3.65−3.56 (m, 1H), 2.87−2.61 (m, 5H), 2.21−2.11 (m, 1H). $^{13}$C NMR (acetone-$d_6$): $\delta$ 174.0, 157.6 (d, $J_{CF}$ = 231 Hz), 148.2, 137.8, 124.7 (d, $J_{CF}$ = 9.3 Hz), 118.4 (d, $J_{CF}$ = 3.5 Hz), 112.5 (d, $J_{CF}$ = 9.7 Hz), 107.9 (d, $J_{CF}$ = 26.1 Hz), 103.0 (d, $J_{CF}$ = 23.4 Hz), 38.9, 35.7, 35.3, 22.9; MS (−APCI) *m*/*z* 232.2 $(M - H)^-$.

Following the procedure described for compound **3**, bromination of the above acid (127 g, 540 mmol) yielded (5-bromo-7-fluoro-1,2,3,4-tetrahydrocyclopenta[*b*]indol-3-yl)acetic acid as a brown solid (117 g, 69%). $^1$H NMR (acetone-$d_6$): $\delta$ 10.84 (br s, 1H), 9.84 (br s, 1H), 7.16−7.09 (m, 2H), 3.67−3.60 (m, 1H), 2.91−2.71 (m, 4H), 2.61 (dd, $J$ = 16.4 and 8 Hz, 1H), 2.27−2.19 (m, 1H). $^{13}$C NMR (acetone-$d_6$): $\delta$ 173.6, 157.0 (d, $J_{CF}$ = 236 Hz), 149.3, 136.0, 125.3 (d, $J_{CF}$ = 10.3 Hz), 120.1 (d, $J_{CF}$ = 4.6 Hz), 110.8 (d, $J_{CF}$ = 29.2 Hz), 103.4 (d, $J_{CF}$ = 12.8 Hz), 102.9 (d, $J_{CF}$ = 23.2 Hz), 38.4, 35.5, 35.3, 23.0. MS (−APCI) *m*/*z* 311.8, 309.8 $(M - H)^-$; Anal. ($C_{13}H_{11}BrNO_2$) C, H, N.

Esterification of the above acid (74.1 g, 240 mmol) with HCl in methanol and alkylation with 4-chlorobenzyl bromide (60 g, 290 mmol) followed by ester hydrolysis, as described previously for compound **4**, provided [5-bromo-4-(4-chlorobenzyl)-7-fluoro-1,2,3,4-tetrahydrocyclopenta[*b*]indol-3-yl]acetic acid as a brown solid (74.1 g, 53% over the three steps). $^1$H NMR (acetone-$d_6$): $\delta$ 10.70 (br s 1H), 7.33 (d, $J$ = 8.4 Hz, 2H), 7.20 (dd, $J$ = 8.9 and 2.3 Hz, 1H), 7.09 (dd, $J$ = 9.0 and 2.3 Hz, 1H), 6.95 (d, $J$ = 8.3 Hz, 2H), 5.92 (d, $J_{AB}$ = 17.8 Hz, 1H), 5.77 (d, $J_{AB}$ = 17.8 Hz, 1H), 3.65−3.60 (m, 1H), 3.00−2.65 (m, 4H), 2.42 (dd, $J$ = 16.1 and 10.1 Hz, 1H), 2.32−2 (m, 1H). $^{13}$C NMR (acetone-$d_6$): $\delta$ 172.1, 156.9 (d, $J_{CF}$ = 237.2 Hz), 151.9, 138.7, 134.1, 132.3, 128.6, 127.5 (d, $J_{CF}$ = 10.2 Hz), 127.2, 119.7 (d, $J_{CF}$ = 4.5 Hz), 113.6 (d, $J_{CF}$ = 28.9 Hz), 103.4 (d, $J_{CF}$ = 22.6 Hz), 102.9 (d, $J_{CF}$ = 12.1 Hz), 48.4, 38.0, 35.5, 35.2, 22.4. MS (−APCI) *m*/*z* 436.3, 434.5 $(M - H)^-$.

**[(3*R*)-5-Bromo-4-(4-chlorobenzyl)-7-fluoro-1,2,3,4-tetrahydrocyclopenta[*b*]indol-3-yl]acetic Acid (11).** A suspension of [5-bromo-4-(4-chlorobenzyl)-7-fluoro-1,2,3,4-tetrahydrocyclopenta[*b*]indol-3-yl]acetic acid (35.3 g, 81 mmol), (S)-(−)-1-(1-naphthyl)ethylamine (13.8 g, 81 mmol), and methanol (650 mL) was heated to reflux in an oil bath and mechanically stirred for 30 min. The resulting suspension was filtered while hot to give 35 g of a white solid consisting of the salt of the desired/undesired enantiomers in 10.5:1 ratio. This material was then heated to reflux in methanol (1 L) for 3 h, and then the suspension was filtered while hot to give 26 g of the corresponding salt. A sample of this material was neutralized and was found to have an enantiomeric purity of 96.9% ee by HPLC analysis [ChiralCel OD column, hexane/2-propanol/acetic acid (95:5:0.1), retention times were 9.6 and 14.6 min (desired)]. Recrystallization of the filtrate from above in ethanol (2.8 L) afforded 21.8 g of a salt, which was treated with 1 N HCl and extracted with ethyl acetate to yield the title enantiomer as a white solid (15.0 g, 42%) in 99% ee. $[\alpha]_D^{21} = +39.2°$ (*c* 1.0, MeOH). $^1$H NMR (acetone-$d_6$): $\delta$ 10.69 (br s, 1H), 7.33 (d, $J$ = 8.3 Hz, 2H), 7.20 (dd, $J$ = 8.9 and 2.1 Hz, 1H), 7.09 (dd, $J$ = 9.0 and 2.2 Hz, 1H), 6.94 (d, $J$ = 8.2 Hz, 2H), 5.92 (d, $J_{AB}$ = 17.8 Hz, 1H), 5.77 (d, $J_{AB}$ = 17.8 Hz, 1H), 3.65−3.62 (m, 1H), 2.95−2.65 (m, 4H), 2.42 (dd, $J$ = 16.1 and 10.1 Hz, 1H), 2.32−2.27 (m, 1H). $^{13}$C NMR (acetone-$d_6$): $\delta$ 172.2, 156.9 (d, $J_{CF}$ = 237 Hz), 151.9, 138.7, 134.1, 132.2, 128.6, 127.5 (d, $J_{CF}$ = 10.2 Hz), 127.2, 119.7 (d, $J_{CF}$ = 4.8 Hz), 113.6 (d, $J_{CF}$ = 28.7 Hz), 103.4 (d, $J_{CF}$ = 22.7 Hz), 102.9 (d, $J_{CF}$ = 12.1 Hz), 48.4, 38.1, 35.6, 35.2, 22.4. MS (−APCI) *m*/*z* 436.2, 434.0 $(M - H)^-$. Anal. ($C_{20}H_{16}BrClNFO_2$) C, H, N.

**[(3*R*)-4-(4-Chlorobenzyl)-7-fluoro-5-acetyl-1,2,3,4-tetrahydrocyclopenta-[*b*]indol-3-yl]acetic Acid (12).** To a DMF (200 mL) solution of the methyl ester of bromide **11** (10.0 g, 22.2 mmol) was added 1-ethoxyvinyltributyltin (10.4 g, 28.8 mmol), and then nitrogen was slowly bubbled through the solution for approximately 5 min. A separate flask was charged with $Pd_2(dba)_3$ (1.0 g, 1.09 mmol), $Ph_3As$ (2.5 g, 8.14 mmol), and DMF (920 mL); nitrogen was bubbled through the solution for several minutes, and then the solution was sonicated for several additional minutes. This catalyst

mixture was then transferred to the reaction flask containing bromide **11** and subsequently heated at 90 °C for 3.5 h. At this time, the reaction was cooled to 50 °C, treated with a 1 N HCl solution (20 mL, 20 mmol), and stirred at this temperature for 2 h. The reaction mixture was then cooled to rt and extracted with EtOAc; the organic phase was washed with water and brine, dried over anhydrous $Na_2SO_4$, and concentrated. The resulting residue was purified by flash chromatography eluting with 30−50% EtOAc/hexanes followed by a second flash purification eluting with 30% EtOAc/hexanes to provide [(3*R*)-4-(4-chlorobenzyl)-7-fluoro-5-acetyl-1,2,3,4-tetrahydrocyclopenta-[*b*]indol-3-yl]acetate as an off-white solid (5.5 g, 60%). $^1$H NMR (acetone-$d_6$): $\delta$ 7.97 (dd, $J$ = 8.9 and 2.5 Hz, 1H), 7.26 (d, $J$ = 8.5 Hz, 2H), 7.21 (dd, $J$ = 12.4 and 2.5 Hz, 1H), 6.79 (d, $J$ = 8.5 Hz, 2H), 5.45 (d, $J_{AB}$ = 18.2 Hz, 1H), 5.37 (d, $J_{AB}$ = 18.2 Hz, 1H), 3.77−3.72 (m, 1H), 3.62 (s, 3H), 2.98−2.75 (m, 4H), 2.54 (dd, $J$ = 15.4 and 9.8 Hz, 1H), 2.36−2.30 (m, 1H), 2.13 (s, 3H). $^{13}$C NMR (acetone-$d_6$): $\delta$ 199.1 (d, $J_{CF}$ = 1.7 Hz), 171.7, 156.2 (d, $J_{CF}$ = 234.9 Hz), 152.2, 137.0, 132.5, 132.4, 128.5, 128.2, 127.7 (d, $J_{CF}$ = 9.8 Hz), 127.6 (d, $J_{CF}$ = 8.0 Hz), 119.0 (d, $J_{CF}$ = 4.6 Hz), 108.9 (d, $J_{CF}$ = 26.7 Hz), 107.5 (d, $J_{CF}$ = 22.8 Hz), 50.9, 49.4, 38.4, 35.5, 35.3, 28.0, 22.6. MS (+APCI) *m*/*z* 416.1, 413.6 $(M + H)^+$; Anal. ($C_{23}H_{21}ClFNO_3$) C, H, N.

The above methyl ester (3.04 g, 7.36 mmol) was taken up in MeOH (50 mL), THF (45 mL), and water (4.5 mL), treated with a 1 N NaOH solution (22 mL, 22 mmol), and stirred at rt for 3 h. At this time, the reaction was acidified with a 1 N HCl solution and extracted with EtOAc; the organic phase was washed with water and brine, dried over anhydrous $Na_2SO_4$, and concentrated. The resulting residue was purified by flash chromatography, eluting with 50−70% EtOAc/hexanes, to provide an off-white solid that was then triturated twice with hexanes (2 × 100 mL) to furnish [(3*R*)-5-acetyl-4-(4-chlorobenzyl)-7-fluoro-1,2,3,4-tetrahydrocyclopenta-[*b*]indol-3-yl]acetic acid as an off-white solid (2.5 g, 90%). $[\alpha]_D^{21}$ = +6.4° (*c* 1.0, MeOH). $^1$H NMR (acetone-$d_6$): $\delta$ 10.9 (br s, 1H), 7.38 (dd, $J$ = 8.9 and 2.5 Hz, 1H), 7.26 (d, $J$ = 8.4 Hz, 2H), 7.21 (dd, $J$ = 9.8 and 2.5 Hz, 1H), 6.71 (d, $J$ = 8.3 Hz, 2H), 5.42 (s, 2H), 3.77−3.73 (m, 1H), 3.01−2.95 (m, 1H), 2.91−2.78 (m, 3H), 2,53 (dd, $J$ = 16.1 and 10.0 Hz, 1H), 2.39−2.27 (m, 1H), 2.14 (s, 3H). $^{13}$C NMR (acetone-$d_6$): $\delta$ 199.8 (d, $J_{CF}$ = 1.5 Hz), 172.9, 156.8 (d, $J_{CF}$ = 235 Hz), 153.0, 137.6, 133.2, 133.0, 129.2, 128.9, 128.4 (d, $J_{CF}$ = 9.6 Hz), 128.2 (d, $J_{CF}$ = 7.0 Hz), 119.6 (d, $J_{CF}$ = 4.4 Hz), 109.6 (d, $J_{CF}$ = 26.5 Hz), 108.1 (d, $J_{CF}$ = 23.0 Hz), 50.1, 38.9, 36.2, 35.9, 28.7, 23.2. MS (−ESI) *m*/*z* 399.9, 397.8 $(M - H)^-$. Anal. ($C_{14}H_{14}BrNO_4S$) calcd: C 66.08, H 4.79, N 3.50. Found: C 65.91, H 4.19, N 3.54.

**[(3*R*)-4-(4-Chlorobenzyl)-7-fluoro-5-(methylsulfonyl)-1,2,3,4-tetrahydrocyclopenta[*b*]indol-3-yl]-acetic Acid (13).** Acid **11** (15.4 g, 35.3 mmol) was first esterified with diazomethane as described above. The sulfonylation was accomplished by mixing the ester thus formed with methanesulfinic acid sodium salt (16.3 g, 160 mmol) and CuI (30.2 g, 159 mmol) in *N*-methylpyrrolidinone (250 mL). The resulting suspension was degassed under a flow of $N_2$, heated to 150 °C, stirred for 3 h, and then cooled to rt. The reaction was quenched by the addition of ethyl acetate (500 mL) and hexanes (500 mL), filtered through a pad of $SiO_2$, eluting with EtOAc, and concentrated. The crude oil was dissolved with EtOAc, washed three times with water and one time with brine, dried over anhydrous $Na_2SO_4$, filtered, and concentrated. The crude material was further purified by flash chromatography eluting with a gradient from 100% toluene to 50% toluene in EtOAc to provide 14 g of material, which was hydrolyzed to the corresponding acid as described above. The title compound was obtained after two successive recrystallizations (150 mL of isopropyl acetate/350 mL of heptane followed by $CH_2Cl_2$/hexanes) as a white solid (9.8 g, 64%). $[\alpha]_D^{21}$ = −29.3° (*c* 1.0, MeOH). $^1$H NMR (acetone-$d_6$): $\delta$ 10.73 (br s, 1H), 7.60 (d, $J$ = 9.0 Hz, 2H), 7.34 (m, 1H), 7.32 (m, 1H), 6.86 (d, $J$ = 8.4 Hz, 2H), 6.31 (d, $J_{AB}$=17.8 Hz, 1H), 5.82 (d, $J_{AB}$ = 17.8 Hz, 1H), 3.48−3.44 (m, 1H), 3.00 (s, 3H), 2.99−2.92 (m, 1H), 2.85−2.70 (m, 3H), 2.44 (dd, $J$=16.1 and 10.2 Hz, 1H), 2.34−2.27 (m, 1H). $^{13}$C NMR (acetone-$d_6$): $\delta$ 173.0, 156.5 (d, $J_{CF}$ = 237 Hz), 153.9, 139.2, 133.7, 133.3, 130.0 (d, $J_{CF}$ = 8.9 Hz), 129.6, 128.2, 127.5 (d, $J_{CF}$ = 7.6 Hz), 122.2 (d, $J_{CF}$ = 4.2 Hz), 112.3 (d, $J_{CF}$ = 29.4 Hz), 111.0 (d, $J_{CF}$ = 22.6 Hz), 50.8, 44.7, 38.6, 36.6, 36.5, 23.3. MS (−ESI) *m*/*z* 435.8, 433.8 $(M - H)^-$. Mp 175 °C. Anal. ($C_{21}H_{19}ClFNO_4S$) C, H, N.

The sodium salt was prepared by the treatment of the above acid (6.45 g, 14.80 mmol) in EtOH (100 mL) with a 1 N NaOH solution (14.8 mL, 14.8 mmol). The organic solvent was removed under vacuum, and the crude solid was dissolved in isopropyl alcohol (1.2 L) under reflux. The final volume was reduced to 500 mL by distillation of the solvent. The sodium salt was crystallized by cooling to rt. The crystalline sodium salt was suspended in $H_2O$, frozen with a dry ice bath, and lyophilized under high vacuum to give the sodium salt of **13** (6.0 g, 88%) as an amorphous white solid. $^1$H NMR (DMSO-$d_6$): $\delta$ 7.63 (dd, $J$ = 8.5 and 2.6 Hz, 1H), 7.47 (dd, $J$ = 9.7 and 2.6 Hz, 1H), 7.33 (d, $J$ = 8.4 Hz, 2H), 6.70 (d, $J$ = 8.4 Hz, 2H), 6.06 (d, $J_{AB}$ = 17.9 Hz, 1H), 5.76 (d, $J_{AB}$ = 17.9 Hz, 1H), 3.37−3.29 (1H, m), 3.08 (3H, s), 2.83−2.77 (1H, m), 2.71−2.66 (1H, m), 2.60−2.53 (1H, m), 2.23−2.15 (2H, m), 1.93 (dd, $J$ = 14.4 and 9.7 Hz, 1H). $^{13}$C NMR ($D_2O$): $\delta$ 180.5, 155.1 (d, $J_{CF}$ = 238.0 Hz), 154.6, 137.8, 132.3, 132.2, 129.2 (d, $J_{CF}$ = 9.0 Hz), 128.6, 126.8, 124.1 (d, $J_{CF}$ = 7.8 Hz), 120.7 (d, $J_{CF}$ = 4.3 Hz), 110.9 (d, $J_{CF}$ = 22.2 Hz), 110.6 (d, $J_{CF}$ = 17.3 Hz), 50.0, 43.7, 42.1, 36.7, 35.4, 22.3. Purity, min 97.2% (method A $t_R$ = 10 min; method B $t_R$ = 9.5 min).

**Acknowledgment.** We thank the Comparative Medicine group at Merck Frosst for their help with the pharmacokinetic studies. We also thank Dr. Daniel Dube for providing the software used in the calculation of the pharmacokinetic parameters reported in this publication. We also thank Tony Pereira, Steve Chang, and Bindhu Karanam for their help with the rat half-life measurement of **13**.

**Supporting Information Available:** Full combustion analysis data along with X-ray crystallographic data of **14** (ORTEP drawing and five tables). This material is available free of charge via the Internet at http://pubs.acs.org.

## References

(1) (a) Howarth, P. H. Histamine and asthma: an appraisal based on specific H1-receptor antagonism. *Clin. Exp. Allergy* **1990**, *20* (Suppl 2), 31−41. (b) White, M. V.; Kaliner, M. A. Mediators of allergic rhinitis. *J. Allergy Clin. Immunol.* **1992**, *90*, 679−704. (c) White, M. V.; Kaliner, M. A. Histamine in allergic diseases. *Clin. Allergy Immunol.* **1996**, *7*, 61−90. (d) Narita, S.; Asakura, K.; Kataura, A. Effects of thromboxane $A_2$ receptor antagonist (Bay u 3405) on nasal symptoms after antigen challenge in sensitized guinea pigs. *Int. Arch. Allergy Immunol.* **1996**, *109*, 161−166.

(2) (a) Chan, C. C.; Dagenais, F.; Firby, P.; Foster, A.; Ford-Hutchinson, A. W. Immediate hypersensitivity reactions in the guinea pig conjunctiva: Studies with a second-generation leukotriene $D_4$ receptor antagonist, MK-571. *Can. J. Physiol. Pharmacol.* **1989**, *67*, 845−850. For reports of montelukast in treating allergic rhinitis, see: (b) Meltzer, E. O.; Malmstrom, K.; Lu, S.; Prenner, B. M.; Wei, L. X.; Weinstein, S. F.; Wolfe, J. D.; Reiss, T. F. Concomitant montelukast and loratadine as treatment for seasonal allergic rhinitis: A randomized, placebo-controlled clinical trial. *J. Allergy Clin. Immunol.* **2000**, *105*, 917−922. (c) Van Adelsberg, J.; Philip, G.; Pedinoff, A. J.; Meltzer, E. O.; Ratner, P. H.; Menten, J.; Reiss, T. F. Montelukast improves symptoms of seasonal allergic rhinitis over a 4-week treatment period. *Allergy* **2003**, *58*, 1268−1276.

(3) Lewis, R. A.; Soter, N. A.; Diamond, P. T.; Austen, K. F.; Oates, J. A.; Roberts, L. J., II. Prostaglandin $D_2$ generation after activation of rat and human mast cells with anti-IgE. *J. Immunol.* **1982**, *129*, 1627−1631.

(4) Park, Y-J.; Baraniuk, J. N. Mechanisms of allergic rhinitis. *Clin. Allergy Immunol.* **2002**, *16*, 275−293.

(5) Doyle, W. J.; Boehm, S.; Skoner, D. P. Physiologic responses to intranasal dose-response challenges with histamine, methacholine, bradykinin, and prostaglandin in adult volunteers with and without nasal allergy. *J. Allergy Clin. Immunol.* **1990**, *86*, 924−935.

(6) Naclerio, R. M.; Meier, H. L.; Kagey-Sobotka, A.; Adkinson, N. F., Jr.; Meyers, D. A.; Norman, P. S.; Lichtenstein, L. M. Mediator release after nasal airway challenge with allergen. *Am. Rev. Respir. Dis.* **1983**, *128*, 597−602.

(7) Matsuoka, T.; Hirata, M.; Tanaka, H.; Takahashi, Y.; Murata, T.; Kabashima, K.; Sugimoto, Y.; Kobayashi, T.; Ushikubi, F.; Aze, Y.; Eguchi, N.; Urade, Y.; Yoshida, N.; Kimura, K.; Mizoguchi, A.; Honda, Y.; Nagai, H.; Narumiya, S. Prostaglandin $D_2$ as a mediator of allergic rhinitis. *Science* **2000**, *287*, 2013−2017.

(8) (a) Trottein, F.; Faveeuw, C.; Gosset, P.; Angeli, V. Role of the D prostanoid receptor 1 in the modulation of immune and inflammatory responses. *Crit. Rev. Immunol.* **2004**, *24* (5), 349−362. (b) Kabashima, K.; Narumiya, S. The DP receptor, allergic inflammation and asthma. *Prostaglandins, Leukotrienes Essent. Fatty Acids* **2003**, *69*, 187−194.

(9) For reports of other DP receptor antagonists, see: (a) Giles, H.; Leff, P.; Bolofo, M. L.; Kelly, M. G.; Robertson, A. D. The classification of prostaglandin DP-receptors in platelets and vasculature using BW A868C, a novel, selective and potent competitive antagonist. *Br. J. Pharmacol*. **1989**, *96*, 291−300. (b) Torisu, K.; Kobayashi, K.; Iwahashi, M.; Egashira, H.; Nakai, Y.; Okada, Y.; Nanbu, F.; Ohuchida, S.; Nakai, H.; Toda, M. Development of a prostaglandin D2 receptor antagonist: Discovery of a new chemical lead. *Eur. J. Med. Chem.* **2005**, *40*, 505−519. (c) Mitsumori, S.; Tsuri, T.; Honma, T.; Hiramatsu, Y.; Okada, T.; Hashizume, H.; Kida, S.; Inagaki, M.; Arimura, A.; Yasui, K.; Asanuma, F.; Kishino, J.; Ohtani, M. Synthesis and biological activity of various derivatives of a novel class of potent, selective, and orally active prostaglandin $D_2$ receptor antagonists. 2. 6,6-Dimethylbicyclo[3.1.1]heptane derivatives. *J. Med. Chem.* **2003**, *46*, 2446−2455. (d) Mitsumori, S.; Tsuri, T.; Honma, T.; Hiramatsu, Y.; Okada, T.; Hashizume, H.; Inagaki, M.; Arimura, A.; Yasui, K.; Asanuma, F.; Kishino, J.; Ohtani, M. Synthesis and biological activity of various derivatives of a novel class of potent, selective, and orally active prostaglandin D2 receptor antagonists. 1. Bicyclo[2.1.1]heptane derivatives. *J. Med. Chem.* **2003**, *46*, 2436−2445. (e) Tsuri, T.; Honma, T.; Hiramatsu, Y.; Okada, T.; Hashizume, H.; Mitsumori, S.; Inagaki, M.; Arimura, A.; Yasui, K.; Asanuma, F.; Kishino, J.; Ohtani, M. Bicyclo[2.1.1]heptane and 6,6-dimethylcyclo[3.1.1]heptane derivatives: Orally active, potent, and selective prostaglandin $D_2$ receptor antagonists. *J. Med. Chem.* **1997**, *40*, 3504−3507.

(10) (a) Sturino, C. F.; Lachance, N.; Boyd, M.; Berthelette, C.; Labelle, M.; Li, L.; Roy, B.; Scheigetz, J.; Tsou, N.; Brideau, C.; Cauchon, E.; Carriere, M.-C.; Denis, D.; Greig, G.; Kargman, S.; Lamontagne, S.; Mathieu, M.-C.; Sawyer, N.; Slipetz, D.; O'Neill, G.; Wang, Z.; Zamboni, R.; Metters, K. M.; Young, R. N. Identification of an indole series of prostaglandin $D_2$ receptor antagonists. *Bioorg. Med. Chem. Lett*. **2006**, *16*, 3043−3048. (b) Berthelette, C.; Lachance, N.; Li, L.; Sturino, C.; Wang, Z. Fluoro substituted cycloalkanoidindoles, compositions containing such compounds and methods of treatment using them. Patent Application WO 2003062200 A2, 2003; *Chem. Abstr*. **2003**, *139*, 149524.

(11) Cheng, K.; Wu, T. -J.; Wu, K. K.; Sturino, C.; Metters, K.; Gottesdiener, K.; Wright, S. D.; Wang, Z.; O'Neill, G.; Lai, E.; Waters, M. G. Antagonism of the prostaglandin $D_2$ receptor1 suppresses nicotinic acid-induced vasodilation in mice and humans. *Proc. Natl. Acad. Sci. U.S.A.* **2006**, *103*, 6682−6687.

(12) Sy, W.-W. Iodination of aromatic amines with iodine and silver sulfate. *Synth. Commun.* **1992**, *22*, 3215−3219.

(13) Chen, C.; Lieberman, D. R.; Larsen, R. D.; Verhoeven, T. R.; Reider, P. J. Syntheses of indoles via a palladium-catalyzed annulation between iodoanilines and ketones. *J. Org. Chem.* **1997**, *62*, 2672−2677.

(14) Lachance, N.; Chan, W. Y. Efficient synthesis of bromocyclopenta-[b]indoles via a bromination-reduction sequences. *J. Heterocycl. Chem.* **2003**, *40*, 289−295.

(15) Gan, T.; Van, Ornum, S. G.; Cook, J. M. The Synthesis of $GABA_A$ active ligands by the Stille process. *Tetrahedron Lett.* **1997**, *38*, 8453−8456.

(16) Beugelmans, R.; Chbani, M. Synthesis of 5- and 6-membered heterocyles by a strategy combining $S_NAr$ and $S_{RN}1$ reactions. *Bull. Soc. Chim. Fr.* **1995**, *132*, 306−313.

(17) (a) Baskin, J. M.; Wang, Z. A mild, convenient synthesis of sulfinic acid salts and sulfonamides from alkyl and aryl halides. *Tetrahedron Lett.* **2002**, *43*, 8479−8483. (b) Baskin, J. M.; Wang, Z. An efficient copper catalyst for the formation of sulfones from sulfinic acid salts and aryl iodides. *Org. Lett.* **2002**, *4*, 4423−4425. (c) Suzuki, H.; Abe, H. Copper-assisted displacement reaction of nonactivated iodoarenes with arenesulfinates. Convenient alternative synthesis of unsymmetrical diaryl sulfones. *Tetrahedron Lett.* **1995**, *36*, 6239−6242.

(18) The absolute stereochemistry of the acetic acid side chain present in antagonists **11**, **12**, and **13** was established to be (*R*) from a single crystal X-ray analysis of the acid intermediate **14**. For the use of **14** in the synthesis of **13**, see: Campos, K. R.; Journet, M.; Lee, S.; Grabowski, E. J. J.; Tillyer, R. D. Asymmetric synthesis of a prostaglandin $D_2$ receptor antagonist. *J. Org. Chem*. **2005**, *70*, 268−274. This structure has been deposited with the Cambridge Crystallographic Data Centre (CCDC601363), and further crystallographic details are available in the Supporting Information.

(19) Abramovitz, M.; Adam, M.; Boie, Y.; Carriere, M.; Denis, D.; Godbout, C.; Lamontagne, S.; Rochette, C.; Sawyer, N.; Tremblay, N. M.; Belley, M.; Gallant, M.; Dufresne, C.; Gareau, Y.; Ruel, R.; Juteau, H.; Labelle, M.; Ouimet, N.; Metters, K. M. The utilization of recombinant prostanoid receptors to determine the affinities and selectivities of prostaglandins and related analogs. *Biochim. Biophys. Acta* **2000**, *1483* (2), 285−293.

(20) Coleman, R. A.; Smith, W. L.; Narumiya, S. International Union of Pharmacology classification of prostanoid receptors: Properties, distribution, and structure of the receptors and their subtypes. *Pharmacol. Rev.* **1994**, *46*, 205−229.

(21)

**Dose Proportionality of Antagonist 6 in Rats**[a]

| dose (mg/kg)[b] | $C_{max}$ ($\mu$M) | $C_{6h}$ ($\mu$M) | AUC 0−6 h ($\mu$M·h) |
|---|---|---|---|
| 10 | 21 | 0.6 | 30 |
| 100 | 31 | 7.0 | 120 |

[a] The corresponding sodium salts were used for these pharmacokinetic studies. $C_{max}$ = maximum concentration reached; $C_{6h}$ = concentration 6 h after dosing; AUC = area under the curve. [b] Vehicle 0.5% methocel; dose volume 10 mL/kg; $n = 2$.

(22) Li, C.; Chauret, N.; Trimble, L. A.; Nicoll-Griffith, D. A.; Silva, J. M.; MacDonald, D.; Perrier, H.; Yergey, J. A.; Parton, T.; Alexander, R. P.; Warrellow, G. J. Investigation of the in vitro metabolism profile of a phospodiesterase-IV inhibitor, CDP-840: Leading to structural optimization. *Drug Metab. Dispos.* **2001**, *29*, 232−241.

(23) Nicoll-Griffith, D. A.; Gupta, N.; Twa, S. P.; Williams, H.; Trimble, L. A.; Yergey, J. A. Verlukast (MK-0679) conjugation with glutathione by rat liver and kidney cytosols and excretion in the bile. *Drug Metab. Dispos.* **1995**, *23*, 1085−1093.

(24) Studies directed at addressing the potential role of transporters in the biliary clearance of antagonists **6** and **7** are currently on-going. Details of these investigations will be reported in due course.

(25) Evans, D. C.; Watt, A. P.; Nicoll-Griffith, D. A.; Baillie, T. A. Drug−protein adducts: An industry perspective on minimizing the potential for drug bioactivation in drug discovery and development. *Chem. Res. Toxicol.* **2004**, *17*, 3−16.

(26) For the radiosynthesis of tritiated **7**, see: Scheigetz, J.; Berthelete, C.; Li, C.; Zamboni, R. J. Base-catalyzed deuterium and tritium labeling of aryl methyl sulfones. *J. Labelled Compd. Radiopharm.* **2004**, *47*, 881−889. The synthesis of tritiated **6** and **13** were accomplished in a similar fashion. The synthesis of $^{14}C$ radiolabeled **11** and **12** will be reported elsewhere.

(27) Day, S. H.; Mao, A.; White, R.; Schulz-Utermoehl, T.; Miller, R.; Beconi, M. G. A semi-automated method for measuring the potential for protein covalent binding in drug discovery. *J. Pharmacol. Toxicol. Methods* **2005**, *52*, 278−285.

(28) The structure of **20**, the enantiomer of **13**, is as follows:

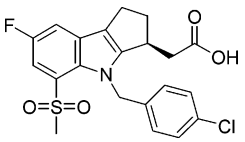


**20**

(29) (a) Hirai, H.; Tanaka, K.; Yoshie, O.; Ogawa, K.; Kenmotsu, K.; Takamori, Y.; Ichimasa, M.; Sugamura, K.; Nakamura, M.; Takano, S.; Nagata, K. Prostaglandin $D_2$ selectively induces chemotaxis in T helper type 2 cells, eosinophils, basophils via seven-transmembrane receptor $CRTH_2$. *J. Exp. Med.* **2001**, *193*, 255−261. (b) Monneret, G.; Gravel, S.; Diamond, M.; Rokach, J.; Powell, W. S. Prostaglandin $D_2$ is a potent chemoattractant for human eosinophils that act via a novel DP receptor. *Blood* **2001**, *98*, 1942−1948. (c) Sawyer, N.; Cauchon, E.; Chateauneuf, A.; Cruz, R. P. G.; Nicholson, D. W.; Metters, K. M.; O'Neill, G. P.; Gervais, F. G. Molecular pharmacology of the human prostagladin $D_2$ receptor, $CRTH_2$. *Br. J. Pharmacol.* **2002**, *137*, 1163−1172.

(30) Abraham, W. M.; Ahmed, A.; Ahmed, T.; Atkins, N. Anderson, P. Pharmacological evaluation of an allergic rhinitis model. *Am. J. Respir. Crit. Care Med*. **1998**, *157*, A616. Jones, T. R.; Savoie, C.;

Robichaud, A.; Sturino, C.; Scheigetz, J.; Lachance, N.; Roy, B.; Boyd, M.; Abraham, W. M. Studies with a DP receptor antagonist in sheep and guinea pig models of allergic rhinitis. *Am. J. Respir. Crit. Care Med.* **2003**, *167*, A218. Abraham, W. M. Modeling of asthma, COPD and cystic fibrosis in sheep. *Pulm. Pharmacol. Ther.*, in press.

(31) No significant inhibition of the major cyctochrome P450 enzymes (1A2, 3A4, 2D6, 2C9) was observed with **13**.

(32) Coleman, R. A.; Humphrey, P. P. A.; Kennedy, I.; Levy, G. P.; Lumley, P. Comparison of the actions of U-46619, a prostaglandin $H_2$ analog, with those of prostaglandin $H_2$ and thromboxane $A_2$ on some isolated smooth muscle preparations. *Br. J. Pharmacol.* **1981**, *73*, 773−778. Liel, N.; Mais, D. E.; Halushka, P. V. Binding of a thromboxane $A_2$/prosataglandin $H_2$ agonist [$^3$H] U46619 to washed human platelets. *Prostaglandins* **1987**, *33*, 789−797.

JM0603668